Plug-and-Play Cooperative Navigation: From Single-Agent Navigation Fields to Graph-Maintaining Distributed MAS Controllers

Dan P. Guralnik, Peter F. Stiller, Federico M. Zegers, *Member, IEEE*, and Warren E. Dixon, *Fellow, IEEE*

***Abstract*—A class of closed-form distributed controllers achieving leader-following in a multiagent system (MAS) with distance-limited communications in a compact obstructed environment is developed: given a user-provided navigation field for a single point agent as an input, the desired MAS PnP ("Plug-and-Play") controller is obtained through a closed-form expression. In particular, cooperative navigation in an environment of arbitrary complexity is achievable whenever an adequate single-agent navigation solution is available. Sufficient conditions on the navigation field in relation to the communication radius are developed, guaranteeing that a prescribed initial graph of agents retains all of its edges while following a leader. In contrast with existing work, the standard radial symmetric interactions among agents are replaced with an asymmetrically rescaled version of the provided navigation field, removing the need for assumptions such as the sphericity or convexity of obstacles, and enabling the switching of the attractive interactions between neighbors on and off as needed. This approach elucidates the tradeoffs between communication range, the size of the MAS, the control effort required for cooperation, and the complexity of navigating in the provided environment. The reliance of the approach on navigation fields enables the use of state-of-the-art sensing-based reactive navigation methods designed for settings with incomplete prior knowledge of the environment and based on a sphere-world model layer. For this reason, two case studies are provided—one of sphere worlds, and the other of topological sphere worlds with star-convex obstacles—comparing different variations of the PnP controller derived from state-of-the-art single-agent navigation fields.**

***Index Terms*—Autonomous networks, consensus control, decentralized control, multi-agent systems, networked control systems, network theory (graphs).**

Manuscript received 23 August 2023; accepted 16 December 2023. Date of publication 25 December 2023; date of current version 30 July 2024. This work was supported in part by AFOSR under Award FA9550-19-1-0169 and Award FA9550-18-1-0109, and in part by the Office of Naval Research under Grant N00014-21-1-2481. *(Corresponding author: Dan Guralnik.)*

Dan P. Guralnik and Warren E. Dixon are with the Department of Mechanical and Aerospace Engineering, University of Florida, Gainesville, FL 32603 USA (e-mail: danguralnik@ufl.edu; wdixon@ufl.edu).

Peter F. Stiller is with the Department of Mathematics, Texas A&M University, College Station, TX 77843 USA (e-mail: p-stiller@tamu.edu).

Federico M. Zegers is with the Johns Hopkins University Applied Physics Laboratory, Laurel, MD 20723 USA (e-mail: federico.zegers@jhuapl.edu).

Digital Object Identifier 10.1109/TAC.2023.3346796

I. Introduction

A. Motivation

MOBILE robotic platforms are increasingly expected to operate in cooperative settings, which creates a need for efficient distributed navigation methods mindful of communication constraints. Nonconvex obstacles in real-life settings increase the tension between task execution and the need for maintaining a connected communication structure by introducing nonconvex inequality constraints into the problem. Safety requirements such as collision-avoidance among agents complicate the problem even further. A standard assumption in the literature on distributed multiagent system (MAS) navigation with connectivity maintenance is that any pair of agents may communicate state information to each other, provided the distance between them does not exceed a prescribed threshold $R > 0$. Such pairs are often referred to as available edges. Despite many advances, the MAS literature has stuck to a set of conservative assumptions simplifying the geometry of obstacles or removing them altogether, while focusing on other aspects and extensions of the problem. Over time, the initial smooth controllers for holonomic single-integrator agents requiring continuous communication [1], [2], [3], [4], [5] gave way to general discussions of graph maintenance such as [6]; to solutions allowing for complex behaviors such as formation reconfiguration [7]; and to challenging contexts such as intermittent communication and actuation [8], [9], [10]; and second order agent dynamics [11]—just to name a few. At the same time, new advances in the literature on single agent reactive navigation based on a recent broad extension [12] of the Rimon-Koditschek navigation paradigm [13] have made reactive navigation possible even with multiple nonconvex obstacles [14], [15]. More refined methods, specialized for the plane, using harmonic functions have also been developed [16], [17]. Following a preliminary conference version [18], this article develops a framework for directly harnessing the capabilities of arbitrary single-agent navigation methods for the purpose of cooperative navigation of a connected MAS, while removing the need for advanced knowledge of the environment beyond what is required for navigation by a single agent using the provided method. The framework introduces a class of extensions of a provided single-agent navigation solution to a multiagent one, along with formal guarantees of communication graph maintenance, making any future single-agent navigation methods immediately applicable in the distributed MAS setting. This "future-proofing" feature is of particular importance in dimension 3 and higher, where single-agent navigation methods are currently largely unavailable for domains that are not topological sphere worlds.[1]

B. Related Work

Assume that the MAS workspace $\Omega \subset \mathbb{R}^d$ is a compact domain with piecewise-smooth boundary.

1) Navigation Functions (NFs): In [20], an NF on Ω with target $x^* \in \mathtt{int}(\Omega)$ is defined as a C^2-smooth[2] function $\varphi : \Omega \to [0, 1]$ such that (a) $\varphi^{-1}(\{1\}) = \partial\Omega$, (b) $\varphi^{-1}(\{0\}) = \{x^*\}$, (c) all the critical points of φ are nondegenerate, and (d) φ has no local minima in $\mathtt{int}(\Omega)$ except for x^*. Then, $\partial\Omega$ is a repelling set of the dynamical system $\dot{x} = \mathfrak{n}(x^*, x) \triangleq -\nabla\varphi(x)$ on Ω, x^* is its unique stable equilibrium, and the complement of the basin of attraction of x^* has zero measure. The connected components $O_1, \ldots, O_b$ of the set $\Omega^* \triangleq \mathbb{R}^d \setminus \Omega$ are usually regarded as obstacles to navigation. This navigation paradigm is desirable due to its built-in guarantee of stability and bounded actuation [13]. The original constructions, known as Rimon-Koditschek navigation functions (RKNFs), took the form

$$\varphi \triangleq \gamma \left(\gamma^k + \prod_{i=1}^{b} \beta_i \right)^{-1/k} \quad (1)$$

where $\gamma : \Omega \to [0, \infty)$ and $\beta_i : \Omega \to [0, \infty)$, $i = 1, \ldots, b$ are C^2-smooth functions with $\gamma^{-1}(0) = \{x^*\}$ and where, for each $i = 1, \ldots, b$, the zero level set of β_i coincides with the boundary ∂O_i of O_i. The function γ may be seen as a cost, while each β_i plays the role of a barrier for the dynamics $\dot{x} = -\nabla\varphi(x)$ in the complement of O_i, preventing its trajectories from exiting the workspace into O_i. Note that no two functions in the collection $\{\gamma, \beta_1, \ldots, \beta_b\}$ have common zeros in this situation. In practice, the functions γ and β_i are often selected as (at least) C^2-smooth functions of $\mathbb{R}^d$ with nonvanishing gradients on $\partial\Omega$ and ∂O_i, respectively.[3] For sphere worlds—workspaces Ω obtained by excavating a disjoint collection of Euclidean balls from a larger Euclidean ball—the cost $\gamma(x) = \|x - x^*\|^2$ and quadratic barrier functions β_i were shown in [20] to give rise to an NF φ, provided $k > 0$ is large enough. These results were extended to star-shaped obstacles via coordinate transformations [13], and broader geometric settings were studied [19], [21], [22], including variations on the algebraic construction of φ, alternative cost functions, and vector fields replacing $\mathfrak{n}(x^*, x) = -\nabla\varphi(x)$. In parallel, recognizing that the RKNF construction and its variants require complete advance knowledge of Ω by the agent, alternative generalizations were developed in results such as [12], [14], [15], and [16] for broader classes of workspaces, known as topological sphere worlds, where the gradient field of a navigation function is replaced by a vector field $\mathfrak{n}(x^*, -)$ computable directly from local sensory information, while retaining the same convergence properties.

2) Graph Maintenance Methods: The established approaches to MAS control with distance-limited communications rely on the graphs $\mathcal{G}_R(\mathbf{x})$, whose vertex set $\mathcal{V}$ indexes the agents and each $p \in \mathcal{V}$ is labeled by the corresponding agent state $x_p \in \mathbb{R}^d$; the edge set $\mathcal{E}_R(\mathbf{x})$ is the set of available edges for the communication range R; and $\mathbf{x} \triangleq (x_p)_{p\in\mathcal{V}}$ denotes the combined MAS state. The graph maintenance (GM) approach focuses on maintaining $\mathcal{E} \subseteq \mathcal{E}_R(\mathbf{x}(t))$ for all $t \geq 0$, provided an initial communication graph $\mathcal{G} = (\mathcal{V}, \mathcal{E})$ with $\mathcal{E} \subseteq \mathcal{E}_R(\mathbf{x}(0))$.

The connectivity maintenance (CM) approach requires that $\mathcal{G}_R(\mathbf{x}(t))$ remain connected for all $t \geq 0$ while allowing the set of available edges to vary over time. This may be achieved, for example, by ensuring that a reduced weighted Laplacian of $\mathcal{G}_R(\mathbf{x})$ remains nonsingular (see, e.g., [2] and [23]), or by seeking to maximize the smallest positive eigenvalue of $\mathcal{G}_R(\mathbf{x})$ subject to task constraints (e.g., [24]). More recent work in this direction, such as [25], applies to a general class of obstacles, through the use of control-barrier functions (CBF). The CM approach is more flexible than GM, as it allows the MAS to switch between communication structures as long as connectivity is maintained. Nevertheless, this article focuses on GM for two reasons. First, GM does not require agents to be continually aware of peers dropping in and out of communication range, instead relying on peer-to-peer communication over a set $\mathcal{E}$ of edges determined a priori. Second, despite the loss of flexibility as compared to CM, GM has the advantage of explicitly acknowledging the underlying switched/hybrid nature of the overarching coordination problem: continuous modes of the MAS are matched with communication protocols (enumerated by graphs), which facilitates a compositional approach to higher-level planning for more complex tasks, as in [26]. The GM literature divides, roughly, into two technical approaches, one applying distributed navigation functions and the other relying on variants of consensus dynamics.

a) GM via distributed navigation functions (DNFs): Introduced in [1], the DNF approach is a fully distributed alternative to NF constructions such as [27]. It was successfully applied to a variety of MAS coordination problems, such as formation control with obstacle/collision avoidance, e.g., [5], [28]. A DNF-based controller has each agent $p \in \mathcal{V}$ descend the p-component $\nabla_p\varphi_p \triangleq \frac{\partial\varphi_p}{\partial x_p}$ of the gradient of a "personal" navigation function φ_p, constructed similarly to the RKNFs of (1), but depending only on state information communicated to agent p by its neighbors in the communication graph $\mathcal{G}$, e.g.,

$$\varphi_p \triangleq \gamma_p \left(\gamma_p^k + \prod_{i} \beta_{p,i} \right)^{-1/k} \quad (2)$$

where each γ_p is a personal cost function, and the $\beta_{p,i}$ are barrier functions representing interactions between agent p and the obstacles $O_1, \ldots, O_b$ for $i = 1, \ldots, b$, as well as other possible mission constraints on the agent, for $i > b$. In this setting, complex interactions among hypersurfaces in the MAS configuration space corresponding to communication constraints, obstacles, collisions, etc., result in significant technical difficulties in establishing the forward invariance of the set of admissible configurations satisfying all the constraints. Convergence from almost all initial conditions is much harder to guarantee than in

[1]With the notable exception of [19], where navigation functions are constructed for topologically complex domains in $\mathbb{R}^3$ such as knot complements, subject to specific curvature conditions.

[2]Originally, Rimon and Koditschek required analyticity, but C^2 smoothness suffices for their results. Further weakening of the assumptions along $\partial\Omega$ is possible as well.

[3]This requirement may be relaxed to the gradients not vanishing almost everywhere [13].

the NF setting: the singular sets $\nabla_p \varphi_p = 0, p \in \mathcal{V}$ are no longer 0-dimensional, and Morse theory cannot be readily invoked. Instead, the common practice is to deploy Lyapunov [1], [5] and dual-Lyapunov [7] methods, e.g., using $\sum_{p\in\mathcal{V}} \varphi_p$ as a candidate (dual) Lyapunov function. Moreover, existing results resist generalization because of their reliance on simplifying assumptions embodied in the dependence of the cost and barrier functions on interagent distances and the distances of agents to the centers of known spherical obstacles.

b) Laplacian-driven GM: Another dominant approach relies on pairwise interactions between neighbors generating closed-loop dynamics of consensus type, e.g.,

$$\dot{\mathbf{x}} = -(\mathbf{L}_w \otimes \mathbf{I}_d)\mathbf{x} + \mathbf{v} \tag{3}$$

where $\mathbf{L}_w : \mathbb{R}^{\mathcal{V}} \to \mathbb{R}^{\mathcal{V}}$ is the weighted Laplace operator with nonnegative symmetric weights satisfying $w_{pq} = 0$ if $pq \notin \mathcal{E}$ and otherwise $w_{pq} = r(\|x_p - x_q\|)$; $r : \mathbb{R}_{\geq 0} \to \mathbb{R}_{\geq 0}$ is often referred to as the edge tension function, which may be designed to fit the task specification; and $(\mathbb{R}^d)^{\mathcal{V}}$ is identified with $\mathbb{R}^{\mathcal{V}} \otimes \mathbb{R}^d$ in the usual way [4], [6], [29] (second-order variants exist as well, e.g., [30]). The role of the first term in (3) and its variants is to ensure a desired degree of connectivity (e.g., simply remaining within communication range [4], or maintaining a desired relative position [3], [30]) by taking advantage of the contractive contribution of this term (each agent is driven toward the weighted baricenter of the positions of its neighbors), whereas the second term $\mathbf{v} = (v_p)_{p\in\mathcal{V}}$ is meant to ensure the overall task, such as target capture, leader-tracking or formation control. Ensuring that the edges of $\mathcal{G}$ are maintained throughout time may then be done by imposing growth conditions on the function $r(\sigma)$ as σ approaches R from below, and leveraging spectral bounds.[4] CM and GM results are often obtained through analysis of the time derivative of a network potential such as the one reviewed below in Section II-B. Similar constructions exist, approaching the problem by superposing attractive and repulsive potentials. For example, in [3], the theory of subharmonic potentials was combined with Rantzer's theorem [31].

More modern techniques relying on CBFs could also be used for incorporating obstacle-avoidance into, e.g., an existing consensus controller [32]. These techniques rely on replacing the reference controller with an approximation selected from a set of safe inputs, which is computed online using barrier certificates. These methods face computational challenges due to the complexity of nonconvex obstacles and the growth of the set of constraints with the size of the network, noting that, similarly to (2), each obstacle-agent pair (i, p) and each $pq \in \mathcal{E}$ contributes at least one constraint. Further difficulties with applying this framework arise when the geometric complexity of obstacles leads to a failure of continuity (or even existence) of the input selection in certain configurations.

[4]Collision avoidance may also be enforced by imposing a growth condition on $r(\sigma)$ as σ approaches R_0 from above, where $R_0 \in (0, R)$ is a distance that is considered safe for a pair of agents, but for this a repulsive field enforced by negative values of r is required. Similarly, obstacle avoidance may be enforced via the introduction of static virtual agents at the centers of obstacles, which results in additional terms on the right-hand side of (3), and the *de-facto* imposition of a spherical obstacles assumption.

C. Contributions

The approach in this article, extending the preliminary work in [18], is to reduce the MAS coordination problem to a single-agent navigation problem, by having the behavior of all agents in the MAS be given by a closed-form formula that takes as input a single navigation solution. For this reason, we refer to this approach as a "plug and play" (PnP) approach. The following notion, generalizing the properties of gradient fields of navigation functions, as detailed in the beginning of Section I-B1, and of other reactive constructions (see, e.g., [22]), serves as the primary input to the PnP controller, enabling us to abstract away from the geometry of any specific class of environments.

Definition 1: Let $\Omega \subset \mathbb{R}^d, d \geq 2$ be a compact domain given as the set of points $z \in \mathbb{R}^d$ with $\beta(z) \geq 0$, where $\beta : \mathbb{R}^d \to \mathbb{R}$ is C^∞-smooth, with $\nabla\beta \neq 0$ almost everywhere in $\partial\Omega$. A navigation field on Ω is a locally Lipschitz continuous map $\mathfrak{n} : \Omega \times \Omega \to \mathbb{R}^d$ satisfying the following conditions for every $y \in \mathtt{int}(\Omega)$:

1) $\langle \mathfrak{n}(y, z), \nabla_z \beta(z)\rangle \geq 0$ everywhere on $\partial\Omega$;
2) $z = y$ is the unique stable equilibrium of $\mathfrak{n}(y, -)$;
3) for almost all initial conditions $x(0) \in \Omega$, the solutions $x(t)$ of $\dot{x} = \mathfrak{n}(y, x)$ converge to y as $t \to \infty$;
4) there is a continuous positive function $\alpha : \Omega \to \mathbb{R}$ such that $\|\mathfrak{n}(y, z)\| \geq \alpha(y)\|y - z\|$ holds for all z in a neighborhood of y.

The emphasis is on the continuous dependence of $\mathfrak{n}(y, z)$ on both the state z and the navigation target y. In other words, we regard $\{\mathfrak{n}(y, -)\}_{y\in\Omega}$ as a uniformly bounded continuous family of locally Lipschitz continuous controllers for a single-integrator agent with dynamics[5] $\dot{x} = u$ and state in Ω, keeping Ω forward invariant (since β is a barrier for $\mathfrak{n}(y, -)$ along $\partial\Omega$), and guaranteeing $\lim_{t\to+\infty} x(t) = y$ for almost all initial conditions $x(0) \in \Omega$, for each fixed y. The PnP distributed MAS controller is constructed from a navigation field $\mathfrak{n}$, and a connected graph $\mathcal{G} = (\mathcal{V}, \mathcal{E})$ as

$$\dot{x}_p = u_p, \quad u_p \triangleq \sum_{q\sim p} \xi^p_q \mathfrak{n}\left(x_q, x_p\right) + v_p \tag{4}$$

where $\xi^p_q(\mathbf{x}) \geq 0$ is a state-dependent gain, $\mathbf{v} = (v_p)_{p\in\mathcal{V}}$ is the task component of the controller, and $q \sim p$ means q goes over all the vertices with $pq \in \mathcal{E}$. Since this article focuses on a single leader $\ell \in \mathcal{V}$ navigating to a prescribed target x^*, the task component is chosen so as to ensure the arrival of the leader at the designated target (see Section III-C for the detailed construction). The coefficients $\xi^p_q(\mathbf{x})$ are nonconstant and asymmetric, as they depend both on $\mathfrak{n}(x_q, x_p)$ and on edge weights $w_{pq} = r(\|x_q - x_p\|)$ obtained using an appropriately designed tension function r. An R-local property of $\mathfrak{n}$, referred to as (R, δ)-goodness (see Definition 2), is identified, which may be thought of as preventing the navigation field from generating overly wasteful motions towards R-close targets. (R, δ)-goodness results in bounds on the difference between the PnP field and the weighted consensus dynamics associated with the specially designed tension function r, enabling a graph maintenance guarantee. For the sake of concreteness, these constructions are applied in the specific setting of a chain of agents with a single leader, where the PnP controller, together with an appropriate choice of $\mathbf{v}$,

[5]Standard extensions are possible, and we focus on the fully actuated case for simplicity.

is shown to guarantee that (a) every edge of the original chain remains available for all time; (b) no agent initialized in $\mathtt{int}(\Omega)$ exits Ω; and (c) the leader's position converges to the target x^* from almost every initial configuration $\mathbf{x}(0) \in \mathtt{int}(\Omega)^{\mathcal{V}}$. The actual result is more general, however, guaranteeing (a)+(b) for any $\mathbf{v} = \mathbf{v}(\mathbf{x})$ that satisfies certain bounds. There are several material differences between (4) and perturbed Laplacian-based dynamics (3). Most notably, the summands $\xi^p_q \mathfrak{n}(x_q, x_p)$, which seem to come in place of the $w_{pq}(x_q - x_p)$ are no longer skew-symmetric as functions of $\mathcal{V} \times \mathcal{V}$. Nevertheless, these alterations are motivated by the following idea for enforcing (b): By the Bony–Brezis theorem,[6] the PnP controller is automatically guaranteed to provide workspace invariance for agent p for as long as $\xi^p_q \geq 0$ for all $q \sim p$ and v_p satisfies $\langle v_p(z), \nabla_z \beta(z) \rangle \geq 0$ along $\partial\Omega$. This leaves us free to design the coefficients ξ^q_p as closed-form functions of $\mathfrak{n}(x_q, x_p)$ in a way that also enforces (a), resulting in a closed-form formula for the desired MAS controller, which only requires the ability for each agent to compute $\{\mathfrak{n}(x_q, x_p)\}_{q \sim p}$ in real time. For comparison, consider the computational complexity of CBF-based GM with obstacle avoidance as discussed in Section I-B2b: each agent is required to compute in real time a continuous selection of the set of safe inputs (usually as the solution to an optimization problem), determined by constraints indexed (at least) by its neighbors and by the smooth facets of all obstacles. Thus, the PnP controller takes advantage of each individual agent's proficiency (the ability to compute $\mathfrak{n}(-, z)$ at any state z) to achieve a drastic reduction in the overall computational burden on each agent of the MAS. An important contribution in excess of those presented in the preliminary version [18] of this article is the systematic extension of the design and analysis of Laplacian and PnP dynamics to nonnegative tension functions r that are allowed to vanish in substantial portions (e.g., whole subintervals) of their domain (see Section III). Results from algebraic connectivity theory (see Appendices A-C and A-D) are applied to the analysis of the time-derivative of the total potential of perturbed weighted consensus dynamics (3), to generate graph-maintenance guarantees for two parametric families of PnP controllers, one characterized by a contractive behavior similar to that of weighted consensus dynamics, and the other characterized by lazy[7] behavior, where neighboring agents at a safe distance do not exert any attractive force on each other (Theorem 2, Section IV). While the former family may be seen as merely a technical extension of the results of [18], the latter represents a step toward minimizing the control effort required for maintaining the communication protocol constraints imposed on the MAS while still achieving the overall navigation task of (a)+(b)+(c) just discussed. The resulting framework may be of interest in other applications, where lower bounds on the Fiedler value of $\mathcal{G}$ and its subgraphs play a role in the Lyapunov analysis of the closed-loop dynamics of the MAS state. Finally, Section IV discusses single-obstacle and multiple-obstacle example settings with appropriate state-of-the-art navigation fields and presents simulation results for the PnP controller in these settings.

[6]More commonly known as Nagumo's Lemma [33, Th. 3.1] in the case where $\partial\Omega$ is smooth, the more general results required for work with the setup of Definition 1 (Ω nonconvex and/or $\partial\Omega$ nonsmooth) are known together as the Bony–Brezis theorem [34, Sec. 2], [35].

[7]Here, we borrow the term from the theory of probability, where a lazy random walk is one that assigns a positive probability to remaining in the same state.

II. Notation and Preliminaries

Henceforth, $\mathcal{V}$ is a nonempty finite set of cardinality N, indexing the set of agents of a MAS with state vectors in $\mathbb{R}^d$, $d \geq 2$. Vectors $\mathbf{x} \triangleq (x_p)_{p\in\mathcal{V}} \in (\mathbb{R}^d)^{\mathcal{V}}$ are referred to as configurations (of the MAS). For $A \subset \mathbb{R}^d$ and $x \in \mathbb{R}^d$, $\|x\|_A \triangleq \inf_{y\in A} \|x - y\|$ is the Euclidean distance of x to A. The closed Euclidean unit ball in $\mathbb{R}^d$ is denoted by $\mathbb{B}^d$. The notation $\|\cdot\|$ refers to the Euclidean norm, and $\|\cdot\|_p$ is the p-norm. If S is a finite set, the standard basis vectors in $\mathbb{R}^S$ are the functions $e_a \in \mathbb{R}^S, a \in S$ defined as $e_a(s) \triangleq \delta_{as} \in \{0, 1\}$, where $\delta_{as} = 1$ if and only if $s = a$. If $T \subseteq S$, then $\mathbb{1}_T \triangleq \sum_{a\in T} e_a \in \mathbb{R}^S$ is the function with a constant value 1 on T, and zero everywhere else in S. For any real-valued function f and $L \in \mathbb{R}$, $[f = L]$, $[f \leq L]$, and $[f \geq L]$ denote the L-level, sublevel, and super-level sets of f in S, respectively.

A. Graphs and Connectivity

The following are the standard notions from graph theory used in this article.

1) Simple Graphs and Subgraphs: For a nonempty set $\mathcal{V}$, the set $\binom{\mathcal{V}}{2}$ is defined as the set of all two-point subsets $pq \triangleq \{p, q\} \subset \mathcal{V}$, $p \neq q$. By a (simple) graph on the vertex set $\mathcal{V}$ we mean a pair $\mathcal{G} = (\mathcal{V}, \mathcal{E})$, where $\mathcal{E} \subseteq \binom{\mathcal{V}}{2}$. By a subgraph of $\mathcal{G} = (\mathcal{V}, \mathcal{E})$ we mean a graph $(\mathcal{V}^*, \mathcal{E}^*)$ with $\mathcal{V}^* \subseteq \mathcal{V}$ and $\mathcal{E}^* \subseteq \mathcal{E}$. For a fixed graph $\mathcal{G} = (\mathcal{V}, \mathcal{E})$, the relation $pq \in \mathcal{E}$ is denoted by $q \sim_{\mathcal{G}} p$, and by $q \sim p$ when there is no risk of ambiguity in determining the relevant $\mathcal{G}$. The degree $d_p(\mathcal{G})$ of $p \in \mathcal{V}$ in $\mathcal{G}$ is the number of $q \in \mathcal{V}$ satisfying $q \sim_{\mathcal{G}} p$. Also, $\Delta(\mathcal{G})$ denotes the maximum degree of a vertex in $\mathcal{G}$.

Example 1: The graph on $\mathcal{V}$ with an edge set $\binom{\mathcal{V}}{2}$ is called the complete graph on $\mathcal{V}$, and denoted by $\mathbb{K}_{\mathcal{V}}$. Let $k \geq 1$ be an integer. Then, the k-path is the graph $\mathbb{P}_k$ with vertex set $\{0, 1, \ldots, k\}$ and with edges $p \sim q$ if and only if $|q - p| = 1$. The vertices 0 and k are called the endpoints of $\mathbb{P}_k$. More generally, a k-path in a graph $\mathcal{G}$ is a subgraph isomorphic to $\mathbb{P}_k$. The number k is referred to as the length of the path.

For any $\varnothing \neq S \subseteq \mathcal{V}$, the subgraph of $\mathcal{G} = (\mathcal{V}, \mathcal{E})$ induced by S is the graph $\mathcal{G}[S] \triangleq (S, \mathcal{E}[S])$, where, by definition, $pq \in \mathcal{E}[S]$ if and only if $pq \in \mathcal{E}$ and $p, q \in S$. We say that S is a k-clique in $\mathcal{G}$ if $k = |S|$ and $\mathcal{G}[S] = \mathbb{K}_S$.

2) Weights on Graphs: A weight κ on $\mathcal{G}$ is a nonnegative symmetric function $\kappa : \mathcal{V} \times \mathcal{V} \to \mathbb{R}_{\geq 0}$, denoted $(p, q) \mapsto \kappa_{pq}$, such that, for all $p, q \in \mathcal{V}$, $\kappa_{pq} \geq 0$ if $pq \in \mathcal{E}$ and $\kappa_{pq} = 0$ otherwise. The weight κ is said to be degenerate, if $\kappa_{pq} = 0$ for some edge $pq \in \mathcal{E}$. For any weight κ, denote by $\mathcal{E}^+_\kappa$ the set of edges $pq \in \mathcal{E}$ with $\kappa_{pq} > 0$. We will also denote $\mathcal{G}^+_\kappa \triangleq (\mathcal{V}, \mathcal{E}^+_\kappa)$ and refer to this subgraph of $\mathcal{G}$ as the support of κ.

3) Walks and Connectivity: A walk of length k in $\mathcal{G}$ from p to q is a sequence $(p_0, \ldots, p_k)$ of vertices satisfying $p_{i-1}p_i \in \mathcal{E}$ for $i = 1, \ldots, k$, and $p_0 = p, p_k = q$. The smallest k admitting a walk from p to q is referred to as the distance from p to q in $\mathcal{G}$ and is denoted by $|p - q|_{\mathcal{G}}$. The quantity $|p - q|_{\mathcal{G}}$ is set to zero when $p = q$ and is set to infinity when there is no path joining p to q. $\mathcal{G}$ is said to be connected, if every $p, q \in \mathcal{V}$ are at finite distance from each other. An equivalence class of the relation $|p - q|_{\mathcal{G}} < \infty$ on $\mathcal{V}$ induces a subgraph called a connected component of $\mathcal{G}$. We denote the set of connected components of $\mathcal{G}$ by $[\![\mathcal{G}]\!]$. An important example arises when a weight w of the kind discussed in Section I-B2b happens to be degenerate on a connected graph

$\mathcal{G}$. Then, the subgraph $\mathcal{G}_w^+$ contains all the vertices of $\mathcal{G}$, but fewer edges, and may become disconnected, with $[\![\mathcal{G}_w^+]\!]$ containing more than one element.

B. Edge Potentials and Perturbed Consensus Dynamics

1) Edge Tension Function and Edge Potentials: Let $r : \mathbb{R}_{\geq 0} \to \mathbb{R}_{\geq 0}$ be a piecewise continuous function with finitely many jumps. We will say that r is nondegenerate if $r(\sigma) > 0$ for all $\sigma \geq 0$. Following [6], the edge potentials $V_{pq} : (\mathbb{R}^d)^{\mathcal{V}} \to \mathbb{R}_{\geq 0}$ with tension r are defined as

$$V_{pq}(\mathbf{x}) \triangleq P(\|x_p - x_q\|), \quad P(\sigma) \triangleq \int_0^\sigma r(s)s\mathtt{d}s \tag{5}$$

for any $p, q \in \mathcal{V}, p \neq q$. This design is chosen to ensure that V_{pq} satisfies the identity

$$\partial V_{pq}/\partial x_p = r(\|x_p - x_q\|)(x_p - x_q) \tag{6}$$

everywhere except for the case when $\|x_q - x_p\|$ is a point of discontinuity for r. When r is nondegenerate, we will refer to the corresponding edge potentials V_{pq} as nondegenerate, and vice versa. Most edge potentials appearing in the literature (e.g., [3], [4]) are covered by this construction, where r is always selected to be continuous and nondegenerate, and often a monotone nondecreasing function.

2) Total Potential and Perturbed Distance-Based Consensus Dynamics: This section recalls crucial facts about dynamics of the type (3) subject to the state-dependent weights $w_{pq} \triangleq r(\|x_p - x_q\|)$. The identity (6) ensures that the total potential and weights

$$V_{\mathcal{G}}(\mathbf{x}) \triangleq \sum_{pq \in \mathcal{E}} V_{pq}(\mathbf{x}), \quad w_{pq} \triangleq r(\|x_q - x_p\|) \tag{7}$$

satisfy the identity [29, Sec. 7.2]

$$\nabla V_{\mathcal{G}}(\mathbf{x}) = 2(\mathbf{L}_w \otimes \mathbf{I}_d)\mathbf{x} \tag{8}$$

while the closed-loop dynamics of (3), together with (8), yield

$$\begin{aligned}\dot{V}_{\mathcal{G}} &= \langle -(\mathbf{L}_w \otimes \mathbf{I}_d)\mathbf{x} + \mathbf{v}, 2(\mathbf{L}_w \otimes \mathbf{I}_d)\mathbf{x}\rangle \\ &= -2\|(\mathbf{L}_w \otimes \mathbf{I}_d)\mathbf{x}_w^\perp\|^2 + 2\langle \mathbf{v}, (\mathbf{L}_w \otimes \mathbf{I}_d)\mathbf{x}_w^\perp\rangle. \end{aligned} \tag{9}$$

This equation lies at the heart of our approach to the design and analysis of PnP controllers, including in the case of degenerate weights (when w_{pq} may equal zero for edges of the graph $\mathcal{G}$). Recall that the vector Laplacian operator $\mathbf{L}_w \otimes \mathbf{I}_d$ is the positive-semidefinite operator on $(\mathbb{R}^d)^{\mathcal{V}}$ given by

$$((\mathbf{L}_w \otimes \mathbf{I}_d)\mathbf{x})_p = \sum_{q \sim p} w_{pq}(x_q - x_p). \tag{10}$$

Since the multiagent literature seldom makes use of weighted Laplacians with degenerate weights, a detailed review of their construction, properties, and other necessary information is provided in the appendices (Appendix A).

III. PnP Controller

Extending the preliminary discussion in Section I-C, this section formally introduces the control objective, design assumptions, basic GM guarantee, and the PnP controller in full detail.

A. Control Objective and Design Assumptions

We are given N agents, with states $x_p \in \mathbb{R}^d, p \in \mathcal{V}$ evolving under $\dot{x}_p = u_p$, where $u_p \in \mathbb{R}^d$, $d \geq 2$ is a continuous control input. The state x_p of each agent is confined to a workspace $\Omega \subset \mathbb{R}^d$ satisfying the assumption of Definition 1. Then, the sublevel set $[\beta \leq 0]$ has finitely many connected components, which are referred to as obstacles.

Two agents are capable of communicating with each other—but are not obliged to do so—whenever $\|x_p - x_q\| \leq R$. Communication in the MAS may only occur along edges of a prescribed connected graph $\mathcal{G} = (\mathcal{V}, \mathcal{E})$. Hence, only initial configurations $\mathbf{x}(0)$ lying in the interior of the domain $\mathscr{C}_R(\mathcal{G})$ are considered, where, for any $s > 0$, one defines

$$\begin{aligned}\mathscr{C}_s(\mathcal{G}) &\triangleq \left\{\mathbf{x} \in \Omega^{\mathcal{V}} : \mathcal{E} \subseteq \mathcal{E}_s(\mathbf{x})\right\}, \\ \mathcal{E}_s(\mathbf{x}) &\triangleq \left\{pq : \|x_p - x_q\| \leq s\right\}.\end{aligned}$$

$\mathcal{E}_s(\mathbf{x})$ is the set of edges available to the MAS at configuration $\mathbf{x}$ for communication over distances not exceeding s.

A single agent $\ell \in \mathcal{V}$ is designated as the leader and tasked with reaching a user-specified target location $x^* \in \mathtt{int}(\Omega)$, while the MAS as a whole is tasked with maintaining the prescribed communication structure $\mathcal{G} = (\mathcal{V}, \mathcal{E})$ for all time: $\mathbf{x}(t) \in \mathscr{C}_R(\mathcal{G})$ is required to hold for all $t \geq 0$. For simplicity, collisions among agents are allowed, and we assume the agents have complete state feedback at all times. Each agent is provided with a means to compute the navigation field $\mathfrak{n}$ on the workspace Ω. In this sense, each agent shares with the others an effective means of navigating Ω towards any target while avoiding all obstacles. Coordination is achieved through the ability of each agent to access the state information of all its neighbors in $\mathcal{G}$, as long as $\mathbf{x}(t) \in \mathscr{C}_R(\mathcal{G})$ holds.

It stands to reason that some navigation fields may vary too much over short distances to provide useful means of navigation—much less coordination. The following definition is used to eliminate navigation fields of this kind from consideration.

Definition 2: Let $\delta \in (0, 1]$. A navigation field $\mathfrak{n}$ on Ω is (R, δ)-good, if every $y, z \in \Omega$ with $\|y - z\| \leq R$ also satisfy

$$\langle \mathfrak{n}(y, z), y - z\rangle \geq \delta \|\mathfrak{n}(y, z)\| \|y - z\|. \tag{11}$$

In other words, a good navigation field is one that is always at a sufficiently acute angle (namely, one whose cosine$\geq \delta$) to the radial field for nearby targets.

B. Weak Invariance Principle for Graph Maintenance

1) General Argument for Graph Maintenance: The following result was presented in [10] and [18], inspired by the analysis in [6]. Here, it is reformulated and extended to fit a broader class of edge tension functions. Note the independence of the new statement from the particular choice of a controller for the MAS. This matters, as distinct versions of the PnP controller are studied in this article.

Theorem 1: Let $V_{\mathcal{G}}$ be the total edge potential obtained via (7), using a piecewise continuous tension function $r : \mathbb{R}_{\geq 0} \to \mathbb{R}_{\geq 0}$ with only finitely many discontinuities of jump type in the interval $[0, \infty)$. Further, let $\varrho \in (0, R]$ satisfy

$$|\mathcal{E}|\, P(\varrho) < P(R). \tag{12}$$

Suppose $\mathbf{x}(t) : \mathbb{R}_{\geq 0} \to \mathtt{Conf}_{\mathcal{V}}(\Omega)$ is continuous and piecewise C^1 with bounded $\dot{\mathbf{x}}(t)$ and $\mathbf{x}(0) \in \mathscr{C}_\varrho(\mathcal{G})$, and suppose $\dot{V}_\mathcal{G} \leq 0$ whenever $\|\Delta\mathbf{x}(t)\|_\infty \in [\varrho, R]$. Then, $\mathbf{x}(t) \in \mathscr{C}_R(\mathcal{G})$ for all time.

Proof: Suppose $\mathbf{x}(t)$ is a trajectory with $\mathbf{x}(0) \in \mathscr{C}_\varrho(\mathcal{G})$ exiting $\mathscr{C}_R(\mathcal{G})$. Let $t_1 \triangleq \inf\{t \in [0,\infty) : \mathbf{x}(t) \notin \mathscr{C}_R(\mathcal{G})\}$ and let $t_0 \triangleq \sup\{t \in [0, t_1) : \mathbf{x}(t) \in \mathscr{C}_\varrho(\mathcal{G})\}$. The assumptions on $\dot{\mathbf{x}}(t)$ and r imply

$$V_\mathcal{G}(t_1) - V_\mathcal{G}(t_0) = \int_{t_0}^{t_1} \dot{V}_\mathcal{G}(t)\mathtt{d}t \leq 0. \tag{13}$$

Since $r \geq 0$, the function P is monotone nondecreasing. Therefore, $\mathbf{x}(t_0) \in \mathscr{C}_\rho(\mathcal{G})$ implies $P(\|x_q(t_0) - x_p(t_0)\|) \leq P(\varrho)$ for all $pq \in \mathcal{E}$, which results in

$$V_\mathcal{G}(t_0) = \sum_{pq\in\mathcal{E}} P(\|x_q(t_0) - x_p(t_0)\|) \leq \sum_{pq\in\mathcal{E}} P(\varrho) = |\mathcal{E}|\, P(\varrho).$$

Applying (12), we obtain $V_\mathcal{G}(t_0) < P(R)$. At the same time, note that $\|x_p(t_1) - x_q(t_1)\| = R$ for at least one edge $pq \in \mathcal{E}$, yielding $P(R) \leq V_\mathcal{G}(t_1)$; hence, $V_\mathcal{G}(t_0) < V_\mathcal{G}(t_1)$, contradicting (13). ■

Considering the proof, the distance between two neighbors $p, q \in \mathcal{V}$ is said to be safe if $0 \leq \|x_p - x_q\| \leq \varrho$, and unsafe if $\varrho < \|x_p - x_q\| \leq R$, keeping in mind that distances greater than R between neighbors are not allowed by our task specification.

2) Example: A Bound for Nondegenerate Edge Potentials: In [6, Prop. 3.2], $\mathcal{G}$ is connected and r is designed as a continuous monotone nondecreasing function satisfying $\mu \leq r(\sigma) \leq r(R)$ for all $\sigma \in [0, R]$, where $\mu > 0$ is a design parameter. Therefore, $\mathbf{x}_w = \mathbf{x}_\mathcal{V}$ and, using (72) and (86), we may continue (9) as

$$\begin{aligned}\dot{V}_\mathcal{G} &= -2\|(\mathbf{L}_w \otimes \mathbf{I}_d)\mathbf{x}_w^\perp\|^2 + 2\langle \mathbf{v}, (\mathbf{L}_w \otimes \mathbf{I}_d)\mathbf{x}_w^\perp\rangle \\ &\leq -2\lambda_2(\mathcal{G}, w)^2\|\mathbf{x}_\mathcal{V}^\perp\|^2 + 2\lambda_N(\mathcal{G}, w)\|\mathbf{x}_\mathcal{V}^\perp\|\|\mathbf{v}\| \\ &\leq -\lambda_2(\mathcal{G}, w)^2\|\Delta\mathbf{x}\|_\infty^2 + 2\lambda_N(\mathcal{G}, w)\sqrt{N}\|\Delta\mathbf{x}\|_\infty\|\mathbf{v}\| \\ &\leq -\mu^2\lambda_2(\mathcal{G})^2\|\Delta\mathbf{x}\|_\infty^2 \\ &\quad + 4\sqrt{N}\Delta(\mathcal{G})r(\|\Delta\mathbf{x}\|_\infty)\|\Delta\mathbf{x}\|_\infty\|\mathbf{v}\|. \end{aligned} \tag{14}$$

Consequently, any $pq \in \mathcal{E}$ with $\|x_p - x_q\| \geq \varrho > 0$ produces

$$\dot{V}_\mathcal{G} \leq -\mu^2\lambda_2(\mathcal{G})^2\varrho^2 + 4\sqrt{N}\Delta(\mathcal{G})r(\|\Delta\mathbf{x}\|_\infty)\|\Delta\mathbf{x}\|_\infty\|\mathbf{v}\|.$$

If, in addition, all $pq \in \mathcal{E}$ have length not exceeding R, then

$$\dot{V}_\mathcal{G} \leq -\mu^2\lambda_2(\mathcal{G})^2\varrho^2 + 4r(R)\Delta(\mathcal{G})\sqrt{N}R\|\mathbf{v}\| \tag{15}$$

enabling the conclusion that $\dot{V}_\mathcal{G}(\mathbf{x}) \leq 0$ for small enough $\|\mathbf{v}\|$, whenever $\|\Delta\mathbf{x}\|_\infty \in [\varrho, R]$. Applying Theorem 1 to any solution $\mathbf{x}(t)$ of (3) with $\mathbf{x}(0) \in \mathscr{C}_\varrho(\mathcal{G})$ reproduces the weak invariance principle of [6, Prop. 3.2].

3) General Bounds for the Total Edge Potential: The presence of a known lower bound μ on the weights is crucial for the argument laid out in Section III-B2, both for enabling the spectral bounds from (86) and for obtaining the negative-definite term in the time derivative of the total edge potential. The following computation sets up the machinery required for analyzing the degenerate case, demonstrating that a more careful spectral analysis always allows one to proceed in a fashion similar to the nondegenerate one. A more fine-tuned analysis of the weighted vector Laplacian $\mathbf{L}_w \otimes \mathbf{I}_d$ is required in the degenerate case, relying on its orthogonal decomposition into the Laplacians of the connected components of the graph $\mathcal{G}_w^+$, which is reviewed in the appendices (Appendix A-D). Combining (9) with (87) and (89) yields

$$\begin{aligned}\dot{V}_\mathcal{G} &= -2\|(\mathbf{L}_w \otimes \mathbf{I}_d)\mathbf{x}_w^\perp\|^2 + 2\langle \mathbf{v}, (\mathbf{L}_w \otimes \mathbf{I}_d)\mathbf{x}_w^\perp\rangle \\ &= -2\sum_{\mathcal{G}^*\in[\![\mathcal{G}_w^+]\!]} \|(\mathbf{L}_{w|_{\mathcal{G}^*}} \otimes \mathbf{I}_d)\mathbf{x}_{\mathcal{V}^*}^\perp\|^2 \\ &\quad + 2\langle \mathbf{v}, (\mathbf{L}_w \otimes \mathbf{I}_d)\mathbf{x}_w^\perp\rangle \end{aligned} \tag{16}$$

$$\begin{aligned} &\leq -2\sum_{\mathcal{G}^*\in[\![\mathcal{G}_w^+]\!]} \lambda_2(\mathcal{G}^*, w|_{\mathcal{G}^*})^2\|\mathbf{x}_{\mathcal{V}^*}^\perp\|^2 \\ &\quad + 2\langle \mathbf{v}, (\mathbf{L}_w \otimes \mathbf{I}_d)\mathbf{x}_w^\perp\rangle. \end{aligned} \tag{17}$$

Equation (16) provides an improvement over the bound provided in (14) by exposing negative-definite terms that were unaccounted for when the tension function was allowed to vanish. In the presence of edges with null weights, the negative-definite term in (14) vanishes, rendering that bound useless for the purpose of invoking Theorem 1. In contrast, any edge with nonzero weight contributes a negative-definite term to (17), corresponding to the connected component of $\mathcal{G}_w^+$ which contains that edge. Continuing from (17) using Cauchy-Schwartz, (75) and (91) yields

$$\begin{aligned}\dot{V}_\mathcal{G} &\leq -2\sum_{\mathcal{G}^*\in[\![\mathcal{G}_w^+]\!]} \lambda_2(\mathcal{G}^*, w|_{\mathcal{G}^*})^2\|\mathbf{x}_{\mathcal{V}^*}^\perp\|^2 \\ &\quad + 2\|(\mathbf{L}_w \otimes \mathbf{I}_d)\mathbf{x}_w^\perp\|\|\mathbf{v}\| \\ &\leq -\sum_{\mathcal{G}^*\in[\![\mathcal{G}_w^+]\!]} \lambda_2(\mathcal{G}^*, w|_{\mathcal{G}^*})^2\|\pi_{\mathcal{V}^*}^1\Delta\mathbf{x}\|_\infty^2 \\ &\quad + 2\|(\mathbf{L}_w \otimes \mathbf{I}_d)\mathbf{x}_w^\perp\|\|\mathbf{v}\| \\ &\leq -\sum_{\mathcal{G}^*\in[\![\mathcal{G}_w^+]\!]} \lambda_2(\mathcal{G}^*, w|_{\mathcal{G}^*})^2\|\pi_{\mathcal{V}^*}^1\Delta\mathbf{x}\|_\infty^2 \\ &\quad + 2\sqrt{N}\lambda_N(\mathcal{G}, w)\|\Delta\mathbf{x}\|_\infty\|\mathbf{v}\| \end{aligned} \tag{18}$$

which is applied in Section IV to the analysis of the PnP controller.

C. Controller Design

Definition 3: Consider the problem formulation of Section III-A, where $\mathcal{G}$ with $|\mathcal{E}| \geq 2$ is fixed in advance and $\mathfrak{n}$ is a provided (R, δ)-good navigation field with a known bound $U \triangleq \sup_{z\in\Omega}\|\mathfrak{n}(x^*, z)\|$. The PnP controller with tension $r : \mathbb{R}_{\geq 0} \to \mathbb{R}_{\geq 0}$ is defined as $\mathbf{u} \triangleq (u_p)_{p\in\mathcal{V}}$

$$u_p(\mathbf{x}) \triangleq \sum_{q\sim p} \xi_q^p\mathfrak{n}_q^p + v_p \tag{19}$$

where $\mathfrak{n}_q^p(\mathbf{x}) \triangleq \mathfrak{n}(x_q, x_p)$, and $\xi_q^p(\mathbf{x}) \triangleq \xi(x_q, x_p)$ with

$$\xi(y, z) \triangleq \frac{r(\|y - z\|)\|y - z\|^2}{\langle \mathfrak{n}(y, z), y - z\rangle} \tag{20}$$

and the task component $\mathbf{v} \triangleq (v_p)_{p\in\mathcal{V}}$ is defined as

$$v_\ell(\mathbf{x}) \triangleq \gamma\mathfrak{n}\,(x^*, x_\ell) - \sum_{q\sim\ell} \xi_q^\ell \mathfrak{n}_q^\ell \tag{21}$$

with $v_p(\mathbf{x}) = 0$ for $p \in \mathcal{V}$, $p \neq \ell$, and $\gamma > 0$ a gain parameter. Though all of the above depend on the choice of the tension function r, we suppress any references to r wherever possible.

Remark 1: Note from (21) that the leader ℓ follows the trajectories of the field $\gamma\mathfrak{n}(x^*, x_\ell)$ without being affected by the other agents. Therefore, the leader is guaranteed to reach x^*, by item 3) of Definition 1. The case where $v_\ell(\mathbf{x}) = \gamma\mathfrak{n}(x^*, x_\ell)$ is also of interest, due to the followers affecting the trajectory of the leader, but will not be addressed in this article.

Remark 2: Note the denominator in (20) is positive whenever $\|y - z\| \leq R$, because $\mathfrak{n}$ is (R, δ)-good. Moreover

$$\|y - z\| \leq R \implies \|\xi(y, z)\mathfrak{n}(y, z)\| \leq \frac{Rr(R)}{\delta} \tag{22}$$

and $\xi(y, z)\mathfrak{n}(y, z)$ is a continuous function of z in a neighborhood of y, by item 4) of Definition 1.

Remark 3: The $\mathfrak{n}(x^*, x_\ell)$ term in v_ℓ may be replaced by a different reference vector field that keeps Ω invariant, implying that applications of the PnP controller are not confined to navigation tasks. Other first-order task specifications are possible, such as the time derivative of a desired path in $\mathtt{int}(\Omega)$ for the leader to follow, transforming the navigation task into a more general leader-following task. The results of this article will be affected by this kind of change only to the extent it affects the bound U.

1) Design of the Tension Function: This article considers two variants of the PnP controller arising from the following design of the tension function:

$$r(s) \triangleq \begin{cases} \mu, & \text{if } s \in [0, \varrho) \\ \mu + \omega(s - \varrho)^{1+\alpha}, & \text{if } s \in [\varrho, R] \\ 0, & \text{if } s \in (R, \infty) \end{cases} \tag{23}$$

where $\mu, \alpha \geq 0$, $\omega > 0$ are parameters.[8] Note that $r(s) \geq \mu$ for all $s \in [0, R]$, in agreement with the role played by μ in Section III-B2.

1) The contractive PnP controller arises when $\mu > 0$, and is characterized by a tendency of the distances between neighboring agents to contract at a rate bounded below by a function of μ. This controller differs only cosmetically from the controller presented in the preliminary conference version [18] of the present article.
2) The lazy PnP controller, obtained when $\mu = 0$, is characterized by the absence of attractive interactions between neighboring agents at distances below the safe distance ϱ.

To present a unified analysis of the WIPs for the two controllers, the following constants are introduced:

$$m \triangleq \frac{R}{\varrho},\; M \triangleq \frac{r(R)}{r(\varrho^*)} \tag{24}$$

where $\varrho^* \in [\varrho, R)$ is selected to equal ϱ in the contractive case, and $\varrho^* > \varrho$ in the lazy case is to be determined with the goal in mind of satisfying (12) with ϱ^* in place of ϱ. Note that $m > 1$ by construction, and that it is best not to impose higher lower bounds on m, so as not to limit the applicability of the WIP by disqualifying values of ϱ that are too close to the communication radius R. By contrast, upper bounds on m are easily imposed by the user without limiting system capabilities. We will henceforth require

$$1 < m \leq \frac{4}{3} < \sqrt{2} \leq \sqrt{|\mathcal{E}|}. \tag{25}$$

Imposing this upper bound on m is tantamount to requiring that $\varrho \geq \frac{3}{4}R$. A direct calculation of the edge potential P yields $P(\sigma) = \frac{\mu}{2}\sigma^2$ if $\sigma \in [0, \varrho]$, and

$$P(\sigma) = \frac{\mu}{2}\sigma^2 + \frac{\omega\,(\sigma - \varrho)^{2+\alpha}}{(2+\alpha)(3+\alpha)}\,((2+\alpha)\sigma + \varrho) \tag{26}$$

for $\sigma \in [\varrho, R]$. Applying the condition in (12) helps determine appropriate parameter values as follows.

a) Parameters for the contractive controller: In the contractive case, μ acts as a gain constant after factoring ω as $\omega = \omega^*\mu$. Condition (12) of the WIP, in its original form, is ensured by selecting an appropriate value of ω^*. Specifically, recalling that $\varrho^* = \varrho$ in this case

$$\frac{P(R)}{P(\varrho^*)} = m^2 + \frac{2\omega^*\varrho^{1+\alpha}\,(m-1)^{2+\alpha}}{(2+\alpha)\,(3+\alpha)}\,((2+\alpha)\,m + 1)$$

and (12), after some algebra, becomes

$$\frac{P(R)}{P(\varrho^*)} > |\mathcal{E}| \iff \omega^* > \frac{(2+\alpha)(3+\alpha)m^{1+\alpha}\left(|\mathcal{E}|-m^2\right)}{2R^{1+\alpha}(m-1)^{2+\alpha}((2+\alpha)m+1)}.$$

Therefore, by $m > 1$ and (25), selecting

$$\omega^* \triangleq \frac{2+\alpha}{2R^{1+\alpha}} \cdot \frac{m^{1+\alpha}\left(|\mathcal{E}| - m^2\right)}{(m-1)^{2+\alpha}} > 0 \tag{27}$$

guarantees the condition (12). At the same time, substituting (27) into (24) yields the bound

$$M \leq 1 + \frac{(2+\alpha)}{2\,(m-1)}\,|\mathcal{E}|\,. \tag{28}$$

b) Parameters for the lazy controller: In the lazy case, ω assumes the role of a gain, and ϱ^* is computed so as to satisfy $P(R)/P(\varrho^*) > |\mathcal{E}|$ while keeping $\varrho^* \in (\varrho, R)$ as large as possible. Some algebraic manipulation reveals that

$$\frac{P(R)}{P(\sigma)} > \frac{(m-1)^{2+\alpha}}{(m^*-1)^{2+\alpha}},\; m^* \triangleq \frac{\sigma}{\varrho}$$

noting that $1 < m^* < m$. As a result, the required inequality is satisfied by selecting

$$\sigma = \varrho^* \triangleq \varrho + \frac{R - \varrho}{|\mathcal{E}|^{1/(2+\alpha)}}. \tag{29}$$

From (23), the value of the tension function at this position is

$$r(\varrho^*) = \omega\,(\varrho^* - \varrho)^{1+\alpha} = \omega\,|\mathcal{E}|^{-\frac{1+\alpha}{2+\alpha}}\,(R - \varrho)^{1+\alpha}\,. \tag{30}$$

Together with $r(R) = \omega(R - \varrho)^{1+\alpha}$, the preceding equality results in

$$M = |\mathcal{E}|^{\frac{1+\alpha}{2+\alpha}} < |\mathcal{E}|\,. \tag{31}$$

[8]Note that $\alpha \geq 0$ is required for $V_{\mathcal{G}}$ to be continuously differentiable, and $\alpha \geq 1$ is required for r to be continuously differentiable. This article focuses on the range $\alpha \in [0, 1]$, in the interest of limiting control effort.

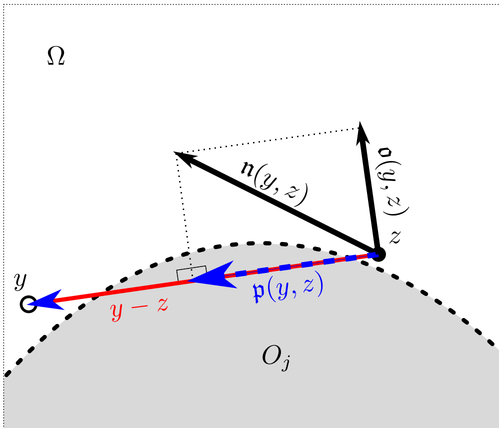

Fig. 1. Orthogonal decomposition of a navigation field.

IV. Communication Graph Maintenance

For the rest of this section, let $\mathfrak{n}$ denote a (R,δ)-good navigation field on Ω, let $\mathcal{G}$ be a connected graph on $\mathcal{V}$, and let $\mathbf{u}$ be the associated PnP controller (Definition 3) with the tension function designed according to one of the options detailed in Section III-C1. The purpose of this section is to obtain conditions under which every trajectory of $\dot{\mathbf{x}}=\mathbf{u}$ with initial condition in $\mathscr{C}_{\varrho^*}(\mathcal{G})$ remains in $\mathscr{C}_R(\mathcal{G})$ for all time (by applying Theorem 1), where $\varrho^*\in[\varrho,R)$ is selected according to Section III-C1.

A. Bounds for the PnP Controller

Consider the decomposition $\mathfrak{n}\triangleq\mathfrak{p}+\mathfrak{o}$ of an (R,δ)-good navigation field $\mathfrak{n}$, where, for $y,z\in\Omega$, $\mathfrak{p}(y,z)\in\operatorname{Span}(y-z)$ and $\mathfrak{o}(y,z)\perp(y-z)$, see Fig. 1. When $\|y-z\|\le R$, this yields

$$\xi(y,z)\mathfrak{n}(y,z)=r(\|y-z\|)(y-z)+\xi(y,z)\mathfrak{o}(y,z)\quad(32)$$

$$\|\mathfrak{o}(y,z)\|\le\sqrt{1-\delta^2}\|\mathfrak{n}(y,z)\|\quad(33)$$

$$\|\xi(y,z)\mathfrak{o}(y,z)\|\le\delta^*r(\|y-z\|)\|y-z\|\le\delta^*r(R)R\quad(34)$$

by (11) and (20), where $\delta^*\triangleq\frac{\sqrt{1-\delta^2}}{\delta}$. Applying these to the PnP field and using the compact notation $\mathfrak{o}_q^p(\mathbf{x})\triangleq\mathfrak{o}(x_q,x_p)$, the following identity over $\mathscr{C}_R(\mathcal{G})$ is obtained:

$$\mathbf{u}=-(\mathbf{L}_w\otimes\mathbf{I}_d)\mathbf{x}+\mathfrak{O}+\mathbf{v},\ \mathfrak{O}_p\triangleq\sum_{q\sim p}\xi_q^p\mathfrak{o}_q^p.\quad(35)$$

Substituting (35) and using (34) yields

$$\|\mathfrak{O}\|^2=\sum_{p\in\mathcal{V}}\left\|\sum_{q\sim p}\xi_p^q\mathfrak{o}_p^q\right\|^2\le\sum_{p\in\mathcal{V}}\left(\sum_{q\sim p}\xi_p^q\|\mathfrak{o}_p^q\|\right)^2$$
$$\le\sum_{p\in\mathcal{V}}(\Delta(\mathcal{G})\delta^*r(R)R)^2=N\left(\Delta(\mathcal{G})\delta^*r(R)R\right)^2$$

which results in

$$\|\mathfrak{O}\|\le\sqrt{N}\Delta(\mathcal{G})\delta^*r(R)R.\quad(36)$$

Using (34) and the triangle inequality, we obtain

$$\|\mathbf{v}\|\le\gamma U+d_\ell\cdot\delta^*r(R)R.\quad(37)$$

Using (88), followed by (91) we also have

$$\|(\mathbf{L}_w\otimes\mathbf{I}_d)\mathbf{x}\|\le\|\mathbf{L}_w\|\|\mathbf{x}_w^\perp\|\le2\Delta(\mathcal{G})r(R)\sqrt{N}R.\quad(38)$$

In particular, the above yield

$$\langle\mathfrak{O},(\mathbf{L}_w\otimes\mathbf{I}_d)\mathbf{x}\rangle\le\|\mathfrak{O}\|\|(\mathbf{L}_w\otimes\mathbf{I}_d)\mathbf{x}\|$$
$$\le2N\Delta(\mathcal{G})^2\delta^*r(R)^2R^2\quad(39)$$

$$\langle\mathbf{v},(\mathbf{L}_w\otimes\mathbf{I}_d)\mathbf{x}\rangle\le2\sqrt{N}\Delta(\mathcal{G})r(R)R\cdot\|\mathbf{v}\|$$
$$\le2\gamma U\sqrt{N}\Delta(\mathcal{G})r(R)R$$
$$+2\sqrt{N}\Delta(\mathcal{G})d_\ell\delta^*r(R)^2R^2.\quad(40)$$

B. Bounds for the Total Potential

Regarding $\mathfrak{O}+\mathbf{v}$ as a perturbation of the weighted Laplacian dynamics in (3) using (35) enables a bound on the time derivative of the total potential (7) under the PnP controller for $\|\Delta\mathbf{x}\|_\infty\in[\varrho^*,R]$ by means of (9)

$$\dot{V}_{\mathcal{G}}=-2\|(\mathbf{L}_w\otimes\mathbf{I}_d)\mathbf{x}\|^2+2\langle\mathfrak{O}+\mathbf{v},(\mathbf{L}_w\otimes\mathbf{I}_d)\mathbf{x}\rangle$$
$$\le-2\|(\mathbf{L}_w\otimes\mathbf{I}_d)\mathbf{x}\|^2$$
$$+4N\delta^*r(R)^2R^2\Delta(\mathcal{G})^2\left(1+\frac{d_\ell}{\Delta(\mathcal{G})\sqrt{N}}\right)$$
$$+4\gamma U\sqrt{N}\Delta(\mathcal{G})r(R)R.\quad(41)$$

Further, (41) may be weakened, using $\frac{d_\ell}{\Delta(\mathcal{G})}\le1$ and $N\ge1$, to a bound that holds for any $\mathcal{G}$, e.g.,

$$\dot{V}_{\mathcal{G}}\le-2\|(\mathbf{L}_w\otimes\mathbf{I}_d)\mathbf{x}\|^2+8N\delta^*r(R)^2R^2\Delta(\mathcal{G})^2$$
$$+4\gamma U\sqrt{N}\Delta(\mathcal{G})r(R)R.\quad(42)$$

For simplicity, all the development hereafter is based on (42), while more precise bounds taking into account specific graph structures could be obtained from (41).

1) Bounds Under the Contractive PnP Controller: In this case, $0<\mu\le r(\sigma)\le r(R)$ for all σ, and (42) yields

$$\dot{V}_{\mathcal{G}}\le-\mu^2\lambda_2(\mathcal{G})^2\varrho^2+8N\delta^*r(R)^2R^2\Delta(\mathcal{G})^2$$
$$+4\gamma U\sqrt{N}\Delta(\mathcal{G})r(R)R$$

where $\varrho^*=\varrho$ in this case. Dividing both sides by $\mu^2\varrho^2$ yields

$$\frac{1}{\mu^2\varrho^2}\dot{V}_{\mathcal{G}}\le-\lambda_2(\mathcal{G})^2+8N\Delta(\mathcal{G})^2\delta^*M^2m^2$$
$$+4\sqrt{N}\Delta(\mathcal{G})Mm\cdot\frac{\gamma U}{\mu\varrho}.\quad(43)$$

Thus, $\dot{V}_{\mathcal{G}}\le0$ under any conditions guaranteeing the inequality

$$8N\Delta(\mathcal{G})^2\delta^*M^2m^2+4\sqrt{N}\Delta(\mathcal{G})Mm\cdot\frac{\gamma U}{\mu\varrho}\le\lambda_2(\mathcal{G})^2\quad(44)$$

and Theorem 1 may be invoked in any such case, leading to the conclusion that $\mathcal{G}$ will be maintained for all time. Note that (44) imposes geometric restrictions on the navigation field, expressed in the requirement that δ^* be sufficiently small, as well as in the requirement that the gain γ be small enough to accommodate (44). For example, one way of securing (44) is to ensure that the triple $(\mathfrak{n},R,\delta)$ satisfies

$$\delta^*\cdot9N\Delta(\mathcal{G})^2M^2m^2\le\lambda_2(\mathcal{G})^2\quad(45)$$

and to then select the gain γ to satisfy

$$\frac{4\gamma U}{\mu\varrho} \leq \delta^*\sqrt{N}\Delta(\mathcal{G})Mm \iff \gamma \leq \frac{\delta^*}{4U}\sqrt{N}\Delta(\mathcal{G})r(R)R.$$

Further developing the right-hand side using (24) and (27) yields

$$\gamma \leq \frac{\mu\delta^*}{4U}\sqrt{N}\Delta(\mathcal{G})R \cdot \left(1 + \frac{2+\alpha}{2} \cdot \frac{|\mathcal{E}| - m^2}{m-1}\right) \tag{46}$$

which, given $\alpha \in [0, 1]$, enables the selection of

$$\gamma \triangleq \frac{\mu\delta^*}{4U}\sqrt{N}\Delta(\mathcal{G})R \cdot \frac{2+\alpha}{6}\,|\mathcal{E}|\,. \tag{47}$$

2) Bounds Under the Lazy PnP Controller: Continuing (42) for the design parameters of the lazy controller using the development from (18), one has $r(\varrho^*) \leq r(\sigma) \leq r(R)$ for all $\sigma \in [\varrho^*, R]$, and hence, for all $\mathbf{x}$ with $\|\Delta\mathbf{x}\|_\infty \in [\varrho^*, R]$

$$\dot{V}_{\mathcal{G}} \leq -\sum_{\mathcal{G}^* \in [\![\mathcal{G}_w^+]\!]} \lambda_2(\mathcal{G}^*, w|_{\mathcal{G}^*})^2 \|\pi^1_{\mathcal{V}^*}\Delta\mathbf{x}\|^2_\infty + 8N\delta^* r(R)^2 R^2 \Delta(\mathcal{G})^2 + 4\gamma U\sqrt{N}\Delta(\mathcal{G})r(R)R$$

where at least one component $\mathcal{G}_0 = (\mathcal{V}_0, \mathcal{E}_0) \in [\![\mathcal{G}_w^+]\!]$ contains an edge pq with $\|x_q - x_p\| \geq \varrho^*$. Therefore, by discarding all the components of $\mathcal{G}_w^+$ not containing pq from the count, the inequality may be continued as

$$\begin{aligned}\dot{V}_{\mathcal{G}} \leq & -\lambda_2(\mathcal{G}_0, w|_{\mathcal{G}_0})^2(\varrho^*)^2 + 8N\delta^* r(R)^2R^2\Delta(\mathcal{G})^2 \\ & + 4\gamma U\sqrt{N}\Delta(\mathcal{G})r(R)R \\ \leq & -\lambda_2(\mathcal{G}_0)^2 r(\varrho^*)^2(\varrho^*)^2 + 8N\delta^* r(R)^2R^2\Delta(\mathcal{G})^2 \\ & + 4\gamma U\sqrt{N}\Delta(\mathcal{G})r(R)R\end{aligned}$$

which, noting that $\frac{R}{\varrho^*} < m$, may further be bounded as

$$\frac{1}{r(\varrho^*)^2(\varrho^*)^2}\dot{V}_{\mathcal{G}} \leq -\lambda_2(\mathcal{G}_0)^2 + 8N\delta^* M^2m^2\Delta(\mathcal{G}) + 4\gamma U\sqrt{N}\Delta(\mathcal{G})Mm$$

producing a condition analogous[9] to (44), where $\lambda_2(\mathcal{G})$ is replaced by $\lambda_2(\mathcal{G}_0)$

$$8N\Delta(\mathcal{G})^2\delta^* M^2m^2 + 4\sqrt{N}\Delta(\mathcal{G})Mm \cdot \frac{\gamma U}{r(\varrho^*)\varrho^*} \leq \lambda_2(\mathcal{G}_0)^2. \tag{48}$$

Requiring again that δ^* be sufficiently small (45), Theorem 1 may be invoked, provided

$$\frac{4\gamma U}{r(\varrho^*)\varrho^*} \leq \delta^*\sqrt{N}\Delta(\mathcal{G})Mm$$

or, equivalently in the lazy case

$$\gamma \leq \frac{\omega\delta^*}{4U}\sqrt{N}\Delta(\mathcal{G})R \cdot (R-\varrho)^{1+\alpha}\left(1 + \frac{m-1}{|\mathcal{E}|^{1/(2+\alpha)}}\right).$$

In particular, selecting the simplified

$$\gamma \triangleq \frac{\omega\delta^*}{4U}\sqrt{N}\Delta(\mathcal{G})R \cdot (R-\varrho)^{1+\alpha} \tag{49}$$

in view of $m > 1$, satisfies this requirement. Note the similarity with (47) in that μ there plays the same role as ω in (49). At the same time, note how the difference $R - \varrho$ figures prominently in (49), as opposed to (47), where it is the size of the graph that matters most for the choice of γ.

[9]Recall that $r(\varrho^*) = \mu$ for the contractive PnP controller.

C. Graph-Maintenance for a Single Chain

In the special case where $\mathcal{G}$ is a path, substituting $\Delta(\mathcal{G}) = 2$ and $\lambda_2(\mathcal{G}) = 4\sin^2\frac{\pi}{2N}$ (see [36]) into the conditions (45) and (47) or (49) (depending on the type of PnP controller being deployed), and invoking Theorem 1 results in the following theorem.

Theorem 2: Suppose $\mathcal{G}$ is an N-path and ℓ is an end of $\mathcal{G}$. Further, suppose that the following holds:

$$\delta^* \cdot M^2m^2 \leq \frac{4}{9N}\sin^4\frac{\pi}{2N}. \tag{50}$$

Then, for any $\gamma \leq \gamma^*$, where

$$\gamma^* \triangleq \frac{\delta^*}{2U}\sqrt{N}R \cdot \begin{cases}\mu \cdot \frac{2+\alpha}{6}\,|\mathcal{E}|\,, & \mu > 0 \\ \omega \cdot R\,(R-\varrho)^{1+\alpha}\,, & \mu = 0\end{cases} \tag{51}$$

any trajectory $\mathbf{x}(t)$ of $\mathbf{u}$ with initial condition $\mathbf{x}(0) \in \mathscr{C}_\varrho(\mathcal{G})$ satisfies the following statements:

1) $\mathbf{x}(t)$ remains in $\mathscr{C}_R(\mathcal{G})$ for all time;
2) $x_\ell(t) \to x^*$ for almost all $x_\ell(0) \in \Omega$.

Proof: In the case of the contractive PnP controller ($\mu > 0$), the assumption in (50) together with the choice of γ^* guarantee the inequality in (44), which is tantamount to $\dot{V}_{\mathcal{G}}(\mathbf{x}(t)) \leq 0$ holding whenever $\|\Delta\mathbf{x}(t)\|_\infty \in [\varrho, R]$. A direct application of Theorem 1 finishes the proof. In the more challenging case of the lazy PnP controller ($\mu = 0$), a crucial observation is that any connected component $\mathcal{G}_0 = (\mathcal{V}_0, \mathcal{E}_0)$ of a subgraph of $\mathcal{G}$ is itself a N_0-path for some $N_0 \leq N$, resulting in

$$\lambda_2(\mathcal{G}_0) = 4\sin^2\frac{\pi}{2N_0} \geq 4\sin^2\frac{\pi}{2N} = \lambda_2(\mathcal{G})$$

and meaning that (50) implies (45). The choice of γ^* then ensures that (48) is satisfied, and $\dot{V}_{\mathcal{G}}(\mathbf{x}(t)) \leq 0$ follows whenever $\|\Delta\mathbf{x}(t)\|_\infty \in [\varrho^*, R]$. Applying Theorem 1 with ϱ^* replacing ϱ allows one to conclude that $\mathbf{x}(t) \in \mathscr{C}_R(\mathcal{G})$ holds for all $t \geq 0$ for all initial conditions $\mathbf{x}(0) \in \mathscr{C}_{\varrho^*}(\mathcal{G})$. In particular, since $\varrho < \varrho^*$, the same is true for all initial conditions $\mathbf{x}(0) \in \mathscr{C}_\varrho(\mathcal{G})$, as desired. ∎

Remark 4: A loose formulation of Theorem 2 is that a short enough chain of agents in a domain whose boundary is not too curved (in comparison to $\frac{1}{R}$) is guaranteed to remain intact for all time, while the leader converges to the desired target. While (51) informs the selection of γ with clear tradeoffs between the size of the network and the PnP gains, (50) reflects a restriction on the pair $(\Omega, \mathfrak{n})$. Observe how smaller values of N allow for larger values of δ^*, which is tantamount to less stringent requirements from the navigation field $\mathfrak{n}$. The right-hand side of (50) only depends on N, decreasing rapidly with N, while $\delta^* = \frac{\sqrt{1-\delta^2}}{\delta}$ only approaches zero as δ approaches 1 (from below). However, δ cannot be treated as a design parameter, since it reflects the quality of the navigation field $\mathfrak{n}$ itself, given R. In turn, $\mathfrak{n}$ depends on the geometry of Ω. At this point, in the case of a smooth $\partial\Omega$, one expects the curvature of the boundary to play a central role in any future detailed analysis: reducing R enables a value of δ nearer to 1, and hence smaller values of δ^*, where the precise

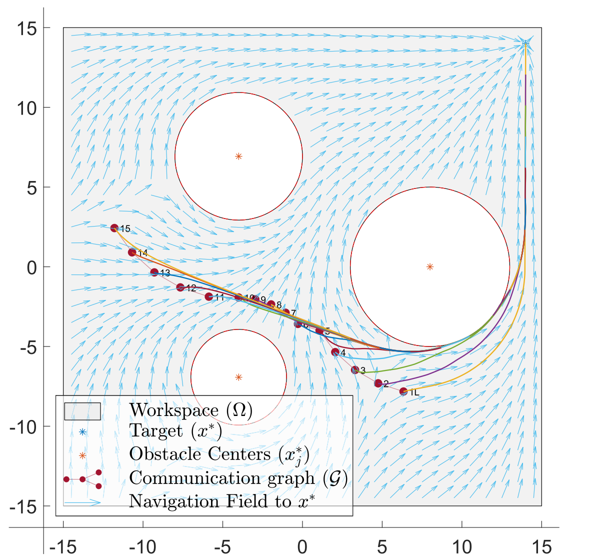

Fig. 2. MAS tracks under a lazy PnP controller in a sphere world: Ω is a rectangle E with three circular disks removed, as described in Section V-A1.

relationship depends on an upper bound on the curvature of $\partial\Omega$. Finally the ratios $m = \frac{R}{\varrho}$ and $M = \frac{r(R)}{r(\varrho^*)}$ may both be regarded as design parameters of the PnP field, while being constrained by the requirements of Theorem 1.

V. Case Studies

Simulations were carried out to compare the contractive PnP controller and the lazy PnP controller. The purpose of this section is to expand the initial study conducted in [18] using state-of-the-art single-agent navigation fields found in the literature, to cover environments with multiple, nonconvex obstacles. A review and analysis of navigation fields for two related classes of environments are included below (navigation in sphere worlds using the method of [12] and navigation in topological sphere worlds where the obstacles are star-convex with smooth boundaries using the method of [14]). Both methods are described in detail to provide a guide to our implementation.[10]

A. Navigation in Sphere Worlds

1) Constructing a Navigation Field: Let $O_i \triangleq x_i^* + \rho_i \mathbb{B}^d$, $i = 1, \ldots, b$, be a collection of pairwise disjoint closed balls, serving as obstacles, contained in a bounded convex environment provided as d-dimensional polytope in the form $E \triangleq \{x \in \mathbb{R}^d : Mx \leq C\}$, where $M = [m_1|\cdots|m_a]^\top \in \mathbb{R}^{a\times d}$ and $C = [c_1, \ldots, c_a]^\top \in \mathbb{R}^a$. Also, let $n_j \triangleq -\frac{m_j}{\|m_j\|}$ be an inward facing normal at any point $z \in \partial E$ satisfying $\langle m_j, z\rangle = c_j$. For each $i = 1, \ldots, b$, let $o_i(z) \triangleq x_i^* + \rho_i(z - x_i^*)$ and let

$$H_i(z) \triangleq \{x \in \mathbb{R}^d : \|x - z\| \leq \|x - o_i(z)\|\} \tag{52}$$

The polytope

$$P(z) \triangleq E \cap \bigcap_{i=1}^{b} H_i(z) \tag{53}$$

may be regarded as a neighborhood of z within which navigation is inherently safe. Following [12], a navigation field $\mathfrak{n}_{\text{sph}}$ on $\Omega \triangleq E \setminus \bigcup_{i=1}^{b} O_i$ is constructed by setting

$$\mathfrak{n}_{\text{sph}}(y, z) \triangleq \pi_z(y) - z \tag{54}$$

where $\pi_z : \mathbb{R}^d \to P(z)$ is the nearest point projection map.

2) Computing the Navigation Field: Developing (52) shows $x \in H_i(z)$ holds if and only if

$$\langle x, x_i^* - z\rangle \leq \frac{\|x_i^* - z\|^2 - \rho_i\|x_i^* - z\|}{2} + \langle z, x_i^* - z\rangle \tag{55}$$

so that $\pi_z(y)$ is the unique solution of the quadratic program

$$\pi_z(y) = \arg\min_x \|x - y\|^2 \text{ s.t. } \begin{cases} Mx \leq C \\ Ax \leq D + Az \end{cases} \tag{56}$$

where $A = A(z) \in \mathbb{R}^{b\times d}$ and $D = D(z) \in \mathbb{R}^b$ are derived from (55), their ith rows satisfying

$$A(z)_i \triangleq (x_i^* - z)^\top \tag{57}$$

$$D(z)_i \triangleq \frac{\|x_i^* - z\|^2 - \rho_i\|x_i^* - z\|}{2}. \tag{58}$$

Using (54), a change of the optimization variable in (56) to $\xi \triangleq x - y$ yields

$$\mathfrak{n}_{sph}(y, z) = \arg\min_\xi \|\xi\|^2 \text{ s.t. } \begin{cases} M\xi \leq C - My \\ A\xi \leq D + A(z - y) \end{cases} \tag{59}$$

which was used to implement $\mathfrak{n}_{\text{sph}}$ in Section V-A4.

3) Verifying the Properties of a Navigation Field: Since establishing the admissibility of $\mathfrak{n}_{\text{sph}}$ as an input to the PnP controller required explicit knowledge of the field's construction, we include a rather detailed analysis of $\mathfrak{n}_{\text{sph}}$ here, for the sake of completeness, as well as to provide a simplified treatment (as compared to [12]). Strictly speaking, Ω does not have a smooth boundary, but, rather, a piecewise smooth one. The properties of a navigation field (Definition 1) are still meaningful in this more general setting, since the nonsmooth points of $\partial\Omega = \partial E \cup \bigcup_{i=1}^{b} \partial O_i$ form a null subset of ∂E. For the rest of this paragraph, let $y \in \texttt{int}(\Omega)$ be fixed. To verify Condition 1 of Definition 1, consider $z \in \partial\Omega$.

1) If $z \in \partial O_i$ for some $i = 1, \ldots, b$ then $z = o_i(z)$ is the unique point of intersection of the convex polytope $P(z)$ with the ball O_i, implying that the radius vector $z - x_i^*$ satisfies $\langle z - x_i^*, x - z\rangle \geq 0$ for all $x \in P(z)$. In particular, for $x = \pi_z(y)$ the desired inequality is obtained.
2) If $z \in \partial E$ then, without loss of generality, there is one and only one $j \in \{1, \ldots, a\}$ such that $\langle m_j, z\rangle = c_j$, with n_j being the inward facing normal to $\partial\Omega$ at z. Since $P(z) \subseteq \{x \in \mathbb{R}^d : \langle m_j, x\rangle \leq c_j\}$, it follows that $\langle n_j, x - z\rangle \geq 0$ for all $x \in P(z)$, and hence also for $x = \pi_z(y)$, as desired.

To verify Conditions 2 and 3 of a navigation field, consider the Lyapunov candidate $V_y(z) \triangleq \|y - z\|^2$. By the convexity of $P(z)$, every $z \in \Omega$ has

$$\langle y - \pi_z(y), z - \pi_z(y)\rangle \leq 0 \tag{60}$$

[10]Code is available at https://github.com/kotmasha-/PnP_multi-agent_navigation.

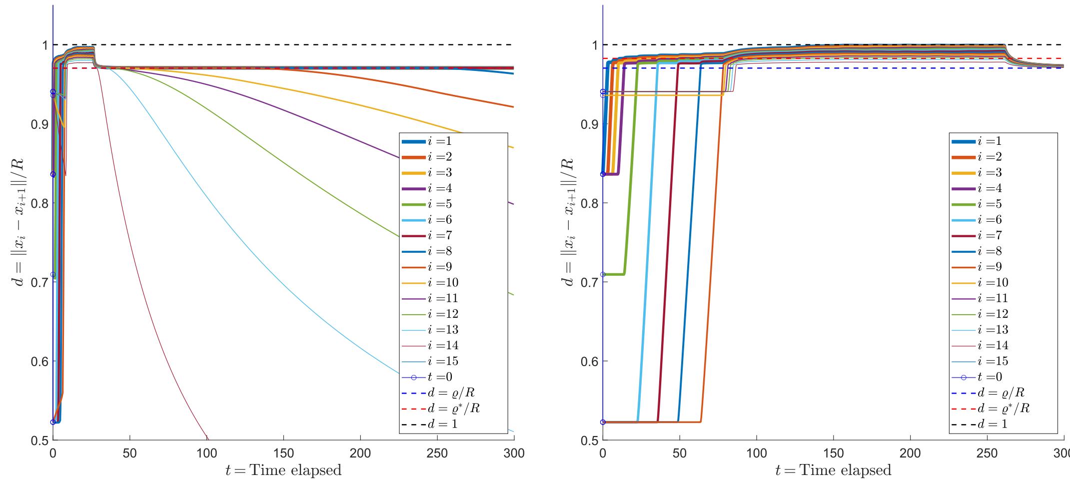

Fig. 3. PnP controllers deployed successfully on a chain of agents in the sphere world from Fig. 2 ($R = 2$): contractive (left, $\mu = 0.015$, $\gamma = 1$) versus lazy (right, $\omega = 220$, $\gamma = 0.1$). The two graphs depict the evolution of normalized distances between consecutive agents over time. Under the lazy controller, distances between neighbors tend to stretch, later decaying to the safe radius ϱ. The contractive controller forces a steady exponential decrease in the interagent distances as the leader nears the target.

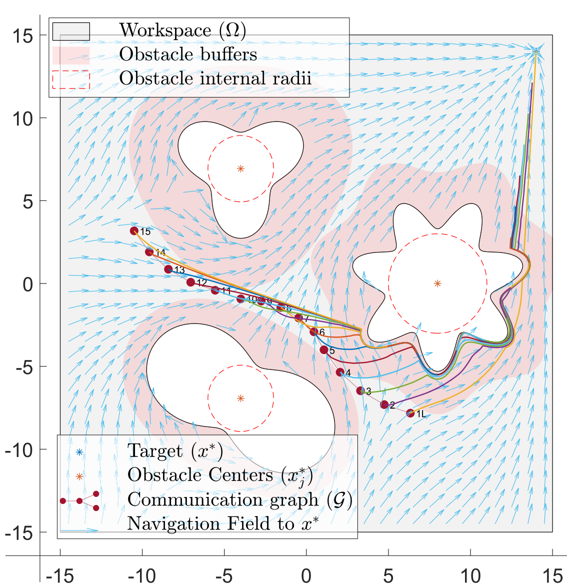

Fig. 4. MAS tracks under a lazy PnP controller in a topological sphere world with star-convex obstacles: Ω is a rectangle E with three deformed disks removed, as described in Section V-B1. Note the pairwise disjoint buffer regions $[\beta_j \leq \varepsilon_j]$ marked in red surrounding the obstacles.

which, after some algebra, results in

$$\langle \nabla_z V_y, \mathfrak{n}_{\text{sph}}(y,z)\rangle \leq -2\|\mathfrak{n}_{\text{sph}}(y,z)\|^2.$$

In other words, $\langle \nabla_z V_y, \mathfrak{n}_{\text{sph}}(y,z)\rangle \leq 0$ for all $z \in \Omega$, with equality only at equilibrium points of $\mathfrak{n}_{\text{sph}}$. Since $z \in \mathtt{int}(P(z))$ whenever $z \in \mathtt{int}(\Omega)$ but $\pi_z(y) \in \{y\} \cup \partial P(z)$ always, equilibrium points of $\mathfrak{n}_{\text{sph}}$ other than y may only lie on the boundary $\partial\Omega$. In fact, they are precisely the points of the form[11] $e_i(y) \triangleq x_i^* + \rho_i \frac{x_i^* - y}{\|x_i^* - y\|}$, $i = 1, \dots, a$. Moreover, direct computation shows that all the directions tangent to ∂O_i at $e_i(y)$ are unstable. To verify Condition 4 of a navigation field, observe that every $y \in \mathtt{int}(\Omega)$ has $r_y > 0$ such that $y + 2r_y\mathbb{B} \subset \Omega$. Then, for every $z \in y + r_y\mathbb{B}$, $y \in P(z)$ must hold, producing $\mathfrak{n}_{sph}(y,z) = y - z$ and meeting the requirement of Condition 4 with $\alpha(y) \equiv 1$. For a discussion of (R,δ)-goodness, see Appendix B.

4) Simulation Results. Sphere World: Simulations were carried out in a sphere world, testing both the contractive and lazy PnP controllers $\mathbf{u}_{\text{sph}}$ based on $\mathfrak{n}_{\text{sph}}$. Fig. 2 shows agent tracks of a typical successful run of a lazy PnP controller on a chain of 15 agents. Fig. 3 compares the results of successful runs of both PnP controllers in this setting in terms of how close each edge of the chain approached breaking. Note how the requirements imposed on the gains γ, μ, ω by Theorem 2 are much more stringent (by several orders of magnitude) than the parameter values used in the simulations. These simulation results also serve as a base-line for comparison with the simulations conducted in Section V-B with nonconvex obstacles.

B. Navigation With Multiple Star-Convex Obstacles

For simplicity of implementation, star-convex obstacles in an environment $E \subset \mathbb{R}^2$ were considered, where E is a finite-sided polytope as in the preceding section. Following [14], obstacles O_j are provided as sublevel sets $[\beta_j \leq 0]$ such that each O_j is star-convex relative to x_j^* and contains a ball $x_j^* + \rho_j\mathbb{B}$. In addition, numbers $\varepsilon_j > 0$ are provided in advance, such that the sets $[\beta_j \leq \varepsilon_j]$ are pairwise disjoint and are all contained in $\mathtt{int}(E)$—see Fig. 4. The workspace is given by $\Omega = E \setminus \bigcup_{j=1}^b O_j$, and a diffeomorphism $h : \Omega \to \Omega_{\text{sph}}$ is computed, where Ω_{sph} is the sphere world $\Omega_{\text{sph}} \triangleq E \setminus \bigcup_{j=1}^b (x_j^* + \rho_j\mathbb{B})$. The map h is constructed as described in Section V-B1, giving rise to the navigation field

$$\mathfrak{n}(y,z) \triangleq Dh(z)^{-1} \cdot \mathfrak{n}_{\text{sph}}\left(h(y), h(z)\right) \tag{61}$$

on Ω, induced from the field $\mathfrak{n}_{\text{sph}}$ on Ω_{sph} by pullback.

Remark 5: Although $\mathfrak{n}$ is conjugate to $\mathfrak{n}_{\text{sph}}$ via the map $h : \Omega \to \Omega_{\text{sph}}$, the map $h^{\mathcal{V}} : \Omega^{\mathcal{V}} \to \Omega_{\text{sph}}^{\mathcal{V}}$ does not conjugate the PnP controller $\mathbf{u}$ based on $\mathfrak{n}$ to the PnP controller $\mathbf{u}_{\text{sph}}$.

[11] Note that $e_i(y)$ is the point of ∂O_i farthest from the target y.

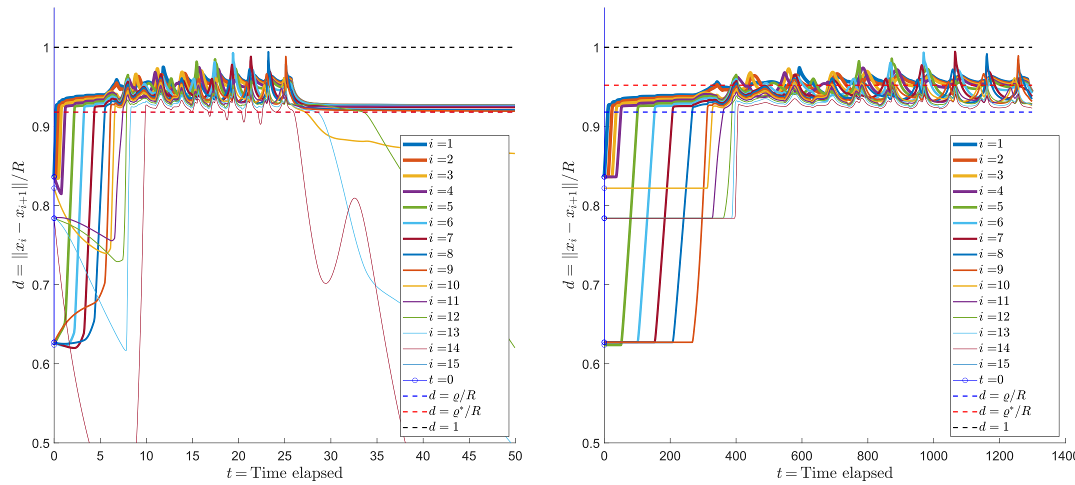

Fig. 5. PnP controllers deployed successfully on a chain of agents in a topological sphere world with nonconvex obstacles. Normalized distances ($R = 2$) between consecutive agents are shown for a contractive PnP controller (left, $\mu = 0.15$, $\gamma = 1$) and a lazy PnP controller (right, $\omega = 25$, $\gamma = 0.02$). A salient feature of the lazy PnP controller is the behavior of the normalized edge-lengths mirroring the interaction between high-curvature segments of the obstacle boundary (the tips of the teeth in the gear-like obstacle depicted in Fig. 4) and the tension between neighboring agents passing in close proximity to those segments (the spikes in the graphs).

1) Construction of the Conjugating Homeomorphism: Following [14, Sec. 3], the map h is constructed as

$$h(z) \triangleq \sigma_d(z)z + \sum_{j=1}^{b} \sigma_j(z) \left(x_j^* + \rho_j \frac{z - x_j^*}{\|z - x_j^*\|} \right) \tag{62}$$

with $\sigma_d \triangleq 1 - \sum_{j=1}^{b} \sigma_j$ and

$$\sigma_j(z) \triangleq \eta_j(\beta_j(z)), \quad \eta_j(s) \triangleq \frac{\zeta(\varepsilon_j - s)}{\zeta(\varepsilon_j)} \tag{63}$$

and where ζ is the standard C^∞ bump function given by $\zeta(s) \triangleq \exp(-1/s)$ for $s > 0$ and otherwise $\zeta(s) = 0$. As a result, $\eta_j'(s) = -(\varepsilon_j - s)^{-2}\eta_j(s)$ for $s < \varepsilon_j$ and $\eta_j'(s) = 0$ for $s \geq \varepsilon_j$. By [14, eq. (13)], the derivative of h is

$$\begin{aligned} Dh(z) &= \sigma_d(z)\mathbf{I}_2 \\ &+ \sum_{j=1}^{b} \frac{\rho_j \sigma_j(z)}{\|z - x_j^*\|} \left(\mathbf{I}_2 - \frac{\left(z - x_j^*\right)\left(z - x_j^*\right)^\top}{\|z - x_j^*\|^2} \right) \\ &+ \sum_{j=1}^{b} \frac{\rho_j - \|z - x_j^*\|}{\|z - x_j^*\|} \left(z - x_j^*\right) D\sigma_j(z) \end{aligned} \tag{64}$$

where $D\sigma_j(z) = \eta_j'(\beta_j(z)) D\beta_j(z)$ takes the form

$$D\sigma_j(z) = -\frac{\sigma_j(z)}{\left(\varepsilon_j - \beta_j(z)\right)^2} D\beta_j(z). \tag{65}$$

Under the conditions that $\nabla\beta_j \neq 0$ along $[\beta_j = 0]$ and that the thickened obstacles $[\beta_j \leq \varepsilon_j]$ are pairwise disjoint, the collection $\Sigma \triangleq \{\sigma_1, \ldots, \sigma_b, \sigma_d\}$ is a C^∞-smooth partition of unity over Ω, and h is, indeed, a diffeomorphism [14, Proposition 1, Assumption 1]. To better showcase the PnP approach, the barrier functions β_j were selected in a way that would allow a direct redesign of the obstacles in the simulation code. The boundary ∂O_j of each obstacle was parametrized as a smooth periodic curve

$$\gamma_j(\theta) \triangleq x_j^* + r_j(\theta)[\cos\theta, \sin\theta]^\top \tag{66}$$

where $r_j(\theta)$ is a C^∞-smooth real-valued function of period 2π satisfying $r_j(\theta) > \rho_j$ for all $\theta \in \mathbb{R}$. The barriers β_j are selected as

$$\beta_j\left(x_j^* + \rho[\cos\theta, \sin\theta]^\top\right) \triangleq \rho^2 - r_j(\theta)^2$$

noting that $\beta_j = 0$ precisely on ∂O_j. The buffer parameters ε_j need to be selected so that the dilated curves $\tilde{\gamma}_j$, $j = 1, \ldots, b$, given in polar coordinates by $\rho = (r_j(\theta)^2 + \varepsilon_j^2)^{1/2}$, form a pairwise-disjoint collection.[12] Differentiating β_j away from its singularity at x_j^*—indeed, $\rho > \rho_j$ for any point of Ω—yields

$$D\beta_j = 2\rho[\cos\theta, \sin\theta]^\top - \frac{2r_j(\theta)r_j'(\theta)}{\rho}[-\sin\theta, \cos\theta]^\top.$$

Thus, (62), (65), and (64) are now implementable.

2) Simulation Results. Nonsphere World: Simulations were carried out in a world with star-convex obstacles with boundaries parametrized as trigonometric polynomials in θ with periods π, $\frac{2\pi}{3}$, $\frac{2\pi}{7}$, see (66), testing both the contractive and lazy PnP controllers with borderline gains. Fig. 4 shows agent tracks under a lazy PnP controller on a chain of 15 agents, while Fig. 5 compares the same lazy controller with a contractive one in terms of interagent distances, as was done earlier for a sphere world in Section V-A4. Note how, again, the requirements imposed on the gains γ, μ, ω by Theorem 2 are more stringent by several orders of magnitude than the parameter values used in these successful simulations.

VI. Conclusion

This article develops generalized edge-weighted Laplacian-based controllers for use in distributed navigation of multiagent systems with distance-limited communication in general obstructed environments. The developed generalization replaces

[12]In simulation, this is an easy condition to verify.

line-of-sight attractive interactions with a provided single-agent navigation field, covering the case of degenerate edge-weights, which allows for reduced attractive interactions along edges that are not at risk of exceeding the communication distance bound. Conditions for applying this method to chains of agents following a leader are derived, and numerical experiments with complex nonconvex and multiple obstacles indicate that much less conservative conditions may be available, depending on additional information about obstacle geometry and/or properties of the provided navigation field. The developed controllers take advantage of the ability of a single agent to navigate the environment to give rise to a family of closed-form, low computational complexity MAS controllers, avoiding the complexities of modern optimization-based cooperative control schemes. The results of this work apply to broader classes of communication structures, where the communication graph $\mathcal{G}$ is not necessarily a path. Most notably, cycles in $\mathcal{G}$ winding around obstacles may present topological obstructions to navigation, preventing the leader from reaching the target without breaking edges of $\mathcal{G}$. It follows that the conditions of Section IV-B cannot be satisfied in such settings, e.g., by a planar network $\mathcal{G}$ containing a cycle that encircles an obstacle, no matter the geometry of the workspace. A deeper understanding of the interactions between such obstructions, curvature conditions on the workspace boundary, the apparent tendency of the PnP contractive field to drive connected components of the MAS to consensus, and the pertinent properties of the provided navigation field, such as Definition 2, is a goal of ongoing research.

Appendix A
Graph Cochains and Graph Laplacians

A. Cochain Spaces of a Graph

Let $\mathcal{G} = (\mathcal{V}, \mathcal{E})$ be a graph. For any subset $\mathcal{O} \subseteq \mathcal{V} \times \mathcal{V}$, the set $\mathcal{O}^{op}$ is defined by setting $(p, q) \in \mathcal{O}^{op}$ if and only if $(q, p) \in \mathcal{O}$. An orientation on $\mathcal{G}$ is a subset $\mathcal{O} \subset \mathcal{V} \times \mathcal{V}$ such that (a) $\mathcal{O} \cap \mathcal{O}^{op} = \varnothing$, and (b) $pq \in \mathcal{E}$ holds if and only if $(p, q) \in \mathcal{O} \cup \mathcal{O}^{op}$. Henceforth, let $\mathcal{O}$ be a fixed orientation. The space $\mathbf{C}^k(\mathcal{G}, \mathbb{R}^n)$ of k-cochains with coefficients in $\mathbb{R}^n$ is the vector space of skew-symmetric $c : \mathcal{V}^{k+1} \to \mathbb{R}^n$ vanishing on $(u_0, \ldots, u_k)$ whenever $\{u_0, \ldots, u_k\}$is not a k-clique in $\mathcal{G}$. This article only considers cochains for $k = 0, 1$ and $n = 1, d$. Inner products on $\mathbf{C}^0(\mathcal{G}, \mathbb{R})$ and $\mathbf{C}^1(\mathcal{G}, \mathbb{R})$ are selected to have the orthonormal bases $\varepsilon^0 \triangleq \{e_p\}_{p\in\mathcal{V}}$ and $\varepsilon^1 \triangleq \{\omega_{p,q}\}_{(p,q)\in\mathcal{O}}$, respectively, where $\omega_{p,q} \triangleq e_{(p,q)} - e_{(q,p)} \in \mathbf{C}^1(\mathcal{G}, \mathbb{R})$. These inner products are extended over $\mathbf{C}^k \triangleq \mathbf{C}^k(\mathcal{G}, \mathbb{R}^d)$ via the identification with $\mathbf{C}^k(\mathcal{G}, \mathbb{R}) \otimes \mathbb{R}^d$, where $\mathbb{R}^d$ is taken with the standard inner product. Further, for $k = 0, 1$, we define

$$\left\| \sum_{f\in\varepsilon^k} f \otimes x_f \right\|_\infty \triangleq \max_{f\in\varepsilon^k} \|x_f\| \tag{67}$$

noting the identification $(x_p)_{p\in\mathcal{V}} \equiv \sum_{p\in\mathcal{V}} e_p \otimes x_p$ of configurations with 0-cochains.

Denoting $\mathbf{C}^0|_S \triangleq \mathtt{Span}(e_a)_{a\in S} \otimes \mathbb{R}^d$ and $\mathbf{C}^1|_S \triangleq \mathtt{Span}(\omega_{p,q})_{pq\in\mathcal{E}[S]} \otimes \mathbb{R}^d$ for all $S \subseteq \mathcal{V}$, let $\pi^{\mathsf{k}}_{\mathsf{S}} : \mathbf{C}^k \to \mathbf{C}^k$ denote the corresponding orthogonal projections of $\mathbf{C}^k$ onto $\mathbf{C}^k|_S$. Then it is clear that, for any $f \in \mathbf{C}^k$, the equality $f = \pi^{\mathsf{k}}_{\mathsf{S}} f + \pi^{\mathsf{k}}_{\mathcal{V}\setminus\mathsf{S}} f$ is an orthogonal decomposition of f, and the following orthogonal sum decomposition holds:

$$\mathbf{C}^k = \bigoplus_{\mathcal{G}^*\in[\![\mathcal{G}]\!]} \mathbf{C}^k|_{\mathcal{V}^*} \cong \bigoplus_{\mathcal{G}^*\in\{\mathcal{G}\}} \mathbf{C}^k(\mathcal{G}^*, \mathbb{R}^d) \tag{68}$$

where $\mathcal{V}^*$ refers to the vertex set of $\mathcal{G}^*$.

B. Agreement Spaces

The agreement subspace of $S \subseteq \mathcal{V}$ is defined as

$$\mathbf{\Delta}_S \triangleq \left\{ \mathbb{1}_S \otimes x : x \in \mathbb{R}^d \right\} \subseteq \mathbf{C}^0 \tag{69}$$

which, when regarded as a subspace of $(\mathbb{R}^d)^\mathcal{V}$, may be identified with the set of all vectors $\mathbf{x}$ with $x_p = 0$ for $p \in \mathcal{V} \setminus S$ and with $x_p = x_q$ for all $p, q \in S$. Let

$$\mathbf{x} \triangleq \mathbf{x}_S + \mathbf{x}_S^\perp + \pi^0_{\mathcal{V}\setminus\mathsf{S}}\mathbf{x} \tag{70}$$

be the orthogonal decomposition[13] of $\mathbf{x}$ with $\mathbf{x}_S \in \mathbf{\Delta}_S$, $\mathbf{x}_S^\perp \in \mathbf{\Delta}_S^\perp \cap \mathbf{C}^0|_S$. Note that $\mathbf{\Delta}_S \subset \mathbf{C}^0|_S$, and $\mathbf{x}_S + \mathbf{x}_S^\perp = \pi^0_{\mathsf{S}}\mathbf{x}$. For any $\mathcal{G} = (\mathcal{V}, \mathcal{E})$ one has the orthogonal decomposition

$$\mathbf{x} = \sum_{\mathcal{G}^*\in[\![\mathcal{G}]\!]} \left(\mathbf{x}_{\mathcal{V}^*} + \mathbf{x}_{\mathcal{V}^*}^\perp\right) \tag{71}$$

in the notation of (68). The following are well-known:

$$\mathbf{x}_\mathcal{V} = \mathbb{1}_\mathcal{V} \otimes \frac{1}{N}\sum_{q\in\mathcal{V}} x_q \tag{72}$$

$$\frac{1}{\sqrt{N}}\|\mathbf{x}_\mathcal{V}^\perp\| \le \|\Delta\mathbf{x}\|_\infty \le \sqrt{2}\|\mathbf{x}_\mathcal{V}^\perp\| \tag{73}$$

where $\Delta\mathbf{x} \in \mathbf{C}^1$ is defined as

$$\Delta\mathbf{x} \triangleq \sum_{(p,q)\in\mathcal{O}} \omega_{p,q} \otimes (x_q - x_p) \equiv (x_q - x_p)_{(p,q)\in\mathcal{O}} \tag{74}$$

and $\|\Delta\mathbf{x}\|_\infty = \max_{(p,q)\in\mathcal{O}} \|x_q - x_p\|$, by (67). Consequently, for the general $S \subseteq \mathcal{V}$

$$\mathbf{x}_S = \mathbb{1}_S \otimes \frac{1}{|S|}\sum_{q\in S} x_q \tag{75}$$

$$\frac{1}{\sqrt{|S|}}\|\mathbf{x}_S^\perp\| \le \|\pi^1_{\mathsf{S}}(\Delta\mathbf{x})\|_\infty \le \sqrt{2}\|\mathbf{x}_S^\perp\| \tag{76}$$

where $\|\pi^1_{\mathsf{S}}(\Delta\mathbf{x})\|_\infty \triangleq \max_{(p,q)\in\mathcal{O}\cap(S\times S)} \|x_q - x_p\|$.

C. Weighted Codifferential and Laplacian

In Section II-B, we introduce a privileged, distance-based weight w on $\mathcal{V}$. The w-weighted graph Laplacian $\mathbf{L}_w : \mathbf{C}^0(\mathcal{G}, \mathbb{R}) \to \mathbf{C}^0(\mathcal{G}, \mathbb{R})$ is the linear operator given by

$$(\mathbf{L}_w g)_p \triangleq \sum_{q\sim p} w_{pq}(g_p - g_q) = w_p g_p - \sum_{q\sim p} w_{pq} g_q \tag{77}$$

[13]Here, $\mathbf{x}_S^\perp$ should not be confused with $(\mathbf{x}_S)^\perp = \mathbf{x}_S^\perp + \pi^0_{\mathcal{V}\setminus\mathsf{S}}\mathbf{x}$.

where $w_p \triangleq \sum_{q\sim p} w_{pq}$. Let $\mathbf{d}_w : \mathbf{C}^0(\mathcal{G},\mathbb{R}) \to \mathbf{C}^1(\mathcal{G},\mathbb{R})$ be defined by

$$(\mathbf{d}_w f)(p,q) \triangleq \sqrt{w_{pq}}\,(f(q)-f(p))\,. \tag{78}$$

Then, observing that $\mathbf{L}_w = \mathbf{d}_w^*\mathbf{d}_w$, one concludes $\mathbf{L}_w$ is positive semidefinite. The vector extensions, $\mathbf{L}_w \otimes \mathbf{I}_d : \mathbf{C}^0 \to \mathbf{C}^0$ and $\mathbf{d}_w \otimes \mathbf{I}_d : \mathbf{C}^0 \to \mathbf{C}^1$, then satisfy the identity

$$\mathbf{L}_w \otimes \mathbf{I}_d = (\mathbf{d}_w \otimes \mathbf{I}_d)^*(\mathbf{d}_w \otimes \mathbf{I}_d) \tag{79}$$

implying that $\mathbf{L}_w \otimes \mathbf{I}_d : \mathbf{C}^0 \to \mathbf{C}^0$ is positive semidefinite and is given by (10). Moreover, the following identity holds for $\mathbf{x},\mathbf{y} \in \mathbf{C}^0$:

$$\langle(\mathbf{L}_w \otimes \mathbf{I}_d)\mathbf{x},\mathbf{y}\rangle = \langle(\mathbf{d}_w \otimes \mathbf{I}_d)\mathbf{x},(\mathbf{d}_w \otimes \mathbf{I}_d)\mathbf{y}\rangle \tag{80}$$

$$= \sum_{(p,q)\in\mathcal{O}} w_{pq}\langle x_q - x_p, y_q - y_p\rangle. \tag{81}$$

In particular, the following also holds for all $\mathbf{x} \in \mathbf{C}^0$:

$$\langle(\mathbf{L}_w \otimes \mathbf{I}_d)\mathbf{x},\mathbf{x}\rangle = \sum_{pq\in\mathcal{E}} w_{pq}\|x_p - x_q\|^2. \tag{82}$$

The eigenvalues of $\mathbf{L}_w$ are nonnegative reals, written as

$$0 = \lambda_1(\mathcal{G},w) \le \lambda_2(\mathcal{G},w) \le \ldots \le \lambda_N(\mathcal{G},w). \tag{83}$$

The constant function $\mathbb{1}_\mathcal{V}$ always satisfies $\mathbf{L}_w\mathbb{1}_\mathcal{V} = 0$. The weight $a \in \mathcal{W}(\mathcal{G})$ with $a_{pq} = 1$ if and only if $pq \in \mathcal{E}$ is referred to as the adjacency matrix of the graph $\mathcal{G}$ and gives rise to the operators $\mathbf{d}_\mathcal{G} \triangleq \mathbf{d}_a, \mathbf{L}_\mathcal{G} \triangleq \mathbf{L}_a$, as well as to $\lambda_k(\mathcal{G}) \triangleq \lambda_k(\mathcal{G},a)$. A weighted Laplacian $\mathbf{L}_w$ may be related to the graph Laplacian $\mathbf{L}_\mathcal{G}$ via the identity

$$\mathbf{L}_w = \mathbf{d}_\mathcal{G}^*\mathbf{O}_w\mathbf{d}_\mathcal{G} \tag{84}$$

where $\mathbf{O}_w$ is the diagonal operator on $\mathbf{C}^1(\mathcal{G},\mathbb{R})$ given by $\mathbf{O}_w\omega_{p,q} = w_{pq}\omega_{p,q}$ for all $(p,q) \in \mathcal{O}$. In the nondegenerate case, if $0 < \theta \le w_{pq} \le \Theta$ for all $pq \in \mathcal{E}$, then $w' \triangleq w - \theta a$ and $w'' \triangleq \Theta a - w$ are weights on $\mathcal{G}$. From $\mathbf{O}_a = \mathbf{I}$ it follows that:

$$\mathbf{0} \le \mathbf{L}_{w'} = \mathbf{d}_\mathcal{G}^*(\mathbf{O}_w - \theta\mathbf{I})\mathbf{d}_\mathcal{G} = \mathbf{L}_w - \theta\mathbf{L}_\mathcal{G}$$

$$\mathbf{0} \le \mathbf{L}_{w''} = \mathbf{d}_\mathcal{G}^*(\Theta\mathbf{I} - \mathbf{O}_w)\mathbf{d}_\mathcal{G} = \Theta\mathbf{L}_\mathcal{G} - \mathbf{L}_w$$

resulting, respectively, in

$$\lambda_2(\mathcal{G},w) \ge \theta\lambda_2(\mathcal{G}) \tag{85}$$

$$\lambda_N(\mathcal{G},w) \le \Theta\lambda_N(\mathcal{G}) \le 2\Theta\Delta(\mathcal{G}) \tag{86}$$

recalling that $\lambda_N(\mathcal{G}) \le 2\Delta(\mathcal{G})$ [36, Th. 2].

D. Laplacians of Disconnected Graphs

When $\mathcal{G} = (\mathcal{V},\mathcal{E})$ is connected and w is a nondegenerate weight on $\mathcal{G}$, the kernel $\ker(\mathbf{L}_w)$ is spanned by $\mathbb{1}_\mathcal{V}$, resulting in $\lambda_2(\mathcal{G},w) > 0$ and in $\ker(\mathbf{L}_w \otimes \mathbf{I}_d)$ coinciding with the agreement subspace $\mathbf{\Delta}_\mathcal{V}$. The general case of a degenerate weight w requires considering the support of w, $\mathcal{G}_w^+$, which may not be connected. For each component $\mathcal{G}^* = (\mathcal{V}^*,\mathcal{E}^*) \in [\![\mathcal{G}_w^+]\!]$ with $N^* = |\mathcal{V}^*|$ vertices, the weight $w|_{\mathcal{G}^*} : \mathcal{V}^* \times \mathcal{V}^* \to \mathbb{R}_{\ge 0}$ given by restricting w is a nondegenerate weight on $\mathcal{G}^*$, and the orthogonal decomposition (68) for the graph $\mathcal{G}_w^+$ is invariant under $\mathbf{L}_w \otimes \mathbf{I}_d$. Thus, $\mathbf{L}_w \otimes \mathbf{I}_d$ coincides with $\mathbf{L}_{w|_{\mathcal{G}^*}} \otimes \mathbf{I}_d$ on each $\mathbf{C}^0|_{\mathcal{V}^*}$, producing

$$\mathbf{L}_w \otimes \mathbf{I}_d = \bigoplus_{\mathcal{G}^*\in[\![\mathcal{G}_w^+]\!]} \mathbf{L}_{w|_{\mathcal{G}^*}} \otimes \mathbf{I}_d. \tag{87}$$

In particular, applying the known results for the connected and nondegenerate case to each individual connected components yields the orthogonal decomposition

$$\ker(\mathbf{L}_w \otimes \mathbf{I}_d) = \bigoplus_{\mathcal{G}^*\in[\![\mathcal{G}_w^+]\!]} \mathbf{\Delta}_{\mathcal{V}^*}. \tag{88}$$

Denoting by $\mathbf{x} \triangleq \mathbf{x}_w + \mathbf{x}_w^\perp$ the orthogonal decomposition with $\mathbf{x}_w \in \ker(\mathbf{L}_w \otimes \mathbf{I}_d)$ and $\mathbf{x}_w^\perp \in \ker(\mathbf{L}_w \otimes \mathbf{I}_d)^\perp = \mathrm{Im}(\mathbf{L}_w \otimes \mathbf{I}_d)$, we obtain from (71) and (75) the orthogonal sum formula

$$\mathbf{x}_w = \sum_{\mathcal{G}^*\in[\![\mathcal{G}_w^+]\!]} \mathbb{1}_{\mathcal{V}^*} \otimes \frac{1}{|\mathcal{V}^*|}\sum_{q\in\mathcal{V}^*} x_q \tag{89}$$

$$\mathbf{x}_w^\perp = \sum_{\mathcal{G}^*\in[\![\mathcal{G}_w^+]\!]} \mathbf{x}_{\mathcal{V}^*}^\perp \tag{90}$$

which, together with (76) yields

$$\|\mathbf{x}_w^\perp\| \le \sqrt{N}\|\Delta\mathbf{x}\|_\infty. \tag{91}$$

Appendix B
Verifying (R,δ)-Goodness in Sphere Worlds

The purpose of this section is to verify that $\mathfrak{n}_{sph}$ is, indeed (R,δ)-good for some $\delta > 0$, provided the obstacles are large enough.[14] Crude lower bounds on δ are studied as functions of the ratios ρ_j/R. We first analyze the case when z is $2R$ away from all obstacles but one. Let $z \in \Omega$ lie at a distance of $2R\nu < R$ from the obstacle O_j. Denote the radius of the obstacle by $\rho_j = \lambda R$. Fixing $y \in \mathtt{int}(\Omega) \cap (z + R\mathbb{B})$, let Π denote the affine plane spanned by z, x_j^*, and y (generically, Π is uniquely determined by this data). Then, $\pi_z(y) \in \Pi$ and a lower bound δ on $\cos(\beta - \alpha)$ is sought, where $\beta \triangleq \angle(\pi_z(y) - z, x_j^* - z)$ and $\alpha \triangleq \angle(y - z, x_j^* - z)$. Note that the value of $\lambda \in (1,\infty)$ is an immutable property of the setting, while the value of $\nu \in (0,1)$ is a property of the point z in relation to $\partial\Omega$, so δ must be provided in terms of R and λ, but not ν. Let p denote a unit vector in the direction of $x_j^* - z$, and let n be a unit vector in an orthogonal direction parallel to Π so that any $y \notin P(z)$ may be written as $y = z + (R\nu + R\phi)p + (R\eta)n$, for $\phi,\eta \ge 0$, as depicted in Fig. 6, making it possible to regard $\cos(\beta - \alpha)$ as a function of (η,ϕ), denoted by $g(\phi,\eta)$

$$g(\phi,\eta) = \frac{\langle(R\phi + R\nu)p + R\eta n, R\nu p + R\eta n\rangle}{\sqrt{(R\phi + R\nu)^2 + (R\eta)^2}\sqrt{(R\phi)^2 + (R\eta)^2}}$$

[14] A restriction of this kind is necessary, because, for example, if R is larger than $2\rho_j$ for some j, then a point $z \in \Omega$ exists such that $O_j \subset \mathtt{int}(z + R\mathbb{B})$, and it becomes impossible to bound $\cos\angle(y - z, \mathfrak{n}_{sph}(y,z))$ for $y \in z + R\mathbb{B}$ from below by a positive number. For example, if $z \in \partial O_j$ then there are points $y \in (z + R\mathbb{B}) \setminus O_j$ arbitrarily close to $x_j^* + \rho_j(x_j^* - z)$, the antipode of z on O_j, for which $\mathfrak{n}_{sph}(y,z)$ is nonzero and tangent to ∂O_j, resulting in an angle $\angle(y - z, \mathfrak{n}_{sph}(y,z))$ arbitrarily close to $\frac{\pi}{2}$.

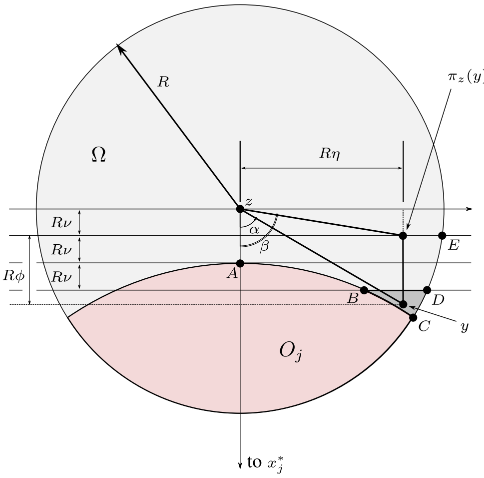

Fig. 6. Verifying (R, δ)-goodness of the sphere-world navigation field $\mathfrak{n}_{sph}$ at distance 2Δ from a single obstacle O_j with center x_j^* and radius $\rho_j = \lambda R$, $\lambda > 1$ (other obstacles are too far away from z to impose constraints on the navigation to R-close targets $y \in z + R\mathbb{B}$). This figure depicts the intersection of the ball $z + R\mathbb{B}$ with the plane containing z, x_j^*, and y, together with the quantities and points of interest (A, B, C, D, E) in the analysis.

$$= \frac{\phi\nu + \nu^2 + \eta^2}{\sqrt{(\phi+\nu)^2 + \eta^2}\sqrt{\nu^2+\eta^2}}. \tag{92}$$

Increasing ϕ while keeping η fixed causes $\cos(\beta - \alpha)$ to decrease, implying $\cos(\beta - \alpha)$ is bounded from below by its values along the union of circular arcs $[A, B, C] \cup [C, D, E]$ as depicted in Fig. 6. Not excluding points of O_j, $g(\phi, \eta)$ is minimized along the circumference of the circle $\Pi \cap (z + R\mathbb{S})$, that is, along the curve in Fig. 6 provided by $(\phi + \nu)^2 + \eta^2 = 1$, producing

$$g(\phi, \eta) \geq \frac{\left(\sqrt{1-\eta^2} - \nu\right)\nu + \nu^2 + \eta^2}{1 \cdot \sqrt{\nu^2 + \eta^2}} \tag{93}$$

which, upon differentiation $d\eta$, may be shown to be minimized when $\nu^2 + \eta^2 = \nu\sqrt{1-\eta^2}$, leading to

$$g(\phi, \eta) \geq \frac{\nu^2 + 2\eta^2}{\sqrt{\nu^2+\eta^2}} = \frac{2(\nu^2+\eta^2) - \nu^2}{\sqrt{\nu^2+\eta^2}}$$
$$\geq 2\sqrt{\nu^2+\eta^2} - \nu^2 \geq \nu(2-\nu).$$

To complement the setting depicted in Fig. 6, $\nu \geq \frac{1}{3}$ is substituted into the preceding inequality, yielding $g(\phi, \eta) \geq \frac{5}{9}$.

Assuming $\nu \in (0, \frac{1}{3})$, a crude bound for points y with $\phi \leq 2\nu$ is obtained from (92) using $g(\phi, \eta) \geq g(2\nu, \eta)$ and neglecting the tern $\phi\nu$ in the numerator, as follows. If $\eta \geq \nu$, then the remaining expression is an increasing function of η in the interval $[0, \infty)$, which yields

$$g(\phi, \eta) \geq \frac{\sqrt{\nu^2+\eta^2}}{\sqrt{(2\nu+\nu)^2+\eta^2}} > \sqrt{\frac{2\nu^2}{10\nu^2}} = \frac{\sqrt{5}}{5} > \frac{11}{25}. \tag{94}$$

If $\eta < \nu$, then $\beta - \alpha \leq \beta < \pi/4$, resulting in $\cos(\beta - \alpha) > \frac{\sqrt{2}}{2} = \frac{\sqrt{2 \cdot 9}}{2 \cdot 3} > \frac{4}{6} = \frac{2}{3}$. Denote by D the point of intersection of ∂O_j with $z + R\mathbb{S}$ in Π, and by B the point of intersection of ∂O_j with the hyperplane $[\phi = 2\nu]$ in Π. Fig. 6 suggests that B does not lie in $z + R\mathbb{B}$ if λ is large enough. In this case, the bound $g(\phi, \eta) > \frac{11}{25}$ holds for all (ϕ, η) by the same argument as in (94). Direct computation shows that $B = (\phi_1, \eta_1) \triangleq (2\nu, \sqrt{2\lambda\nu - \nu^2})$ and $D = (2\nu, \sqrt{1 - 9\nu^2})$ in (ϕ, η) coordinates. Thus, $B \in z + R\mathbb{B}$ if and only if $2\lambda\nu - \nu^2 \leq 1 - (3\nu)^2$, and a lower bound on $g(\phi, \eta)$ along the arc BCD of the boundary of $(z + R\mathbb{B}) \cap \Omega$ is still needed. If $\eta_1 \geq 3\nu$ then $\alpha \geq \pi/4$ forcing $\cos(\beta - \alpha) > \frac{2}{3}$ again, this time due to $\beta - \alpha \leq \pi/2 - \alpha \leq \pi/4$. The condition for this to happen is $2\lambda\nu - \nu^2 \geq 9\nu^2$, or, equivalently, $\lambda \geq 5\nu$. This inequality could be enforced by demanding that $\lambda > 2$. Thus, $\mathfrak{n}_{\text{sph}}$ is $(R, \frac{11}{25})$-good at every point $z \in \Omega$ such that $z + R\mathbb{B}$ intersects at most one obstacle, provided all obstacles have radii at least $2R$. Better bounds are possible with a more careful analysis. In the multiple obstacles setting, note how the same bounds apply if the clearance between obstacles is at least $3R$. In the more general case, a lower bound on δ in the presence of multiple obstacles may be assembled from the individual bounds using Jung's theorem on the sphere [37]. Thus, it is important to note in conclusion of this section that, even in the best-case scenario of Ω being a sphere world, it is currently unrealistic to expect a navigation field to be (R, δ)-good with values of δ near unity, as required by (50). This makes the simulation results in Section V-A4 even more important, as they lend support to the conjecture that more refined bounds on $\|\mathfrak{D}\|$ than those of (36) may exist, obviating the need in the stringent restrictions on δ posed by Theorem 2.

Acknowledgment

Any opinions, findings and conclusions, or recommendations expressed in this material are those of the author(s) and do not necessarily reflect the views of sponsoring agencies.

References

[1] D. V. Dimarogonas, S. G. Loizou, K. J. Kyriakopoulos, and M. M. Zavlanos, "A feedback stabilization and collision avoidance scheme for multiple independent non-point agents," *Automatica*, vol. 42, no. 2, pp. 229–243, 2006.

[2] M. M. Zavlanos and G. J. Pappas, "Potential fields for maintaining connectivity of mobile networks," *IEEE Trans. Robot.*, vol. 23, no. 4, pp. 812–816, Aug. 2007.

[3] D. V. Dimarogonas and K. H. Johansson, "Analysis of robot navigation schemes using Rantzer's dual Lyapunov theorem," in *Proc. Amer. Control Conf.*, 2008, pp. 201–206.

[4] M. Ji and M. Egerstedt, "Distributed coordination control of multiagent systems while preserving connectedness," *IEEE Trans. Robot.*, vol. 23, no. 4, pp. 693–703, Aug. 2007.

[5] Z. Kan, A. Dani, J. M. Shea, and W. E. Dixon, "Network connectivity preserving formation stabilization and obstacle avoidance via a decentralized controller," *IEEE Trans. Autom. Control*, vol. 57, no. 7, pp. 1827–1832, Jul. 2012.

[6] D. Boskos and D. V. Dimarogonas, "Robustness and invariance of connectivity maintenance control for multiagent systems," *SIAM J. Control Optim.*, vol. 55, no. 3, pp. 1887–1914, 2017.

[7] Z. Kan, L. Navaravong, J. Shea, E. Pasiliao, and W. E. Dixon, "Graph matching based formation reconfiguration of networked agents with connectivity maintenance," *IEEE Trans. Control Netw. Syst.*, vol. 2, no. 1, pp. 24–35, Mar. 2015.

[8] Y. Fan and G. Hu, "Connectivity-preserving rendezvous of multi-agent systems with event-triggered controllers," in *Proc. IEEE Conf. Decis. Control*, 2015, pp. 234–239.

[9] X. Yi, J. Wei, D. V. Dimarogonas, and K. H. Johansson, “Formation control for multi-agent systems with connectivity preservation and event-triggered controllers,” *IFAC-PapersOnLine*, vol. 50, no. 1, pp. 9367–9373, 2017.

[10] F. M. Zegers, D. P. Guralnik, and W. E. Dixon, “Event/self-triggered multi-agent system rendezvous with graph maintenance,” in *Proc. IEEE Conf. Decis. Control*, 2021, pp. 1886–1891.

[11] Y. Dong and S. Xu, “Rendezvous with connectivity preservation problem of linear multiagent systems via parallel event-triggered control strategies,” *IEEE Trans. Cybern.*, vol. 52, no. 5, pp. 2725–2734, May 2020.

[12] O. Arslan and D. E. Koditschek, “Sensor-based reactive navigation in unknown convex sphere worlds,” *Int. J. Robot. Res.*, vol. 38, no. 2/3, pp. 196–223, 2019.

[13] E. Rimon and D. E. Koditschek, “Exact robot navigation using artificial potential functions,” *IEEE Trans. Robot. Autom.*, vol. 8, no. 5, pp. 501–518, Oct. 1992.

[14] V. Vasilopoulos and D. E. Koditschek, “Reactive navigation in partially known non-convex environments,” in *Proc. Int. Workshop Algorithmic Found. Robot.*, 2018, pp. 406–421.

[15] V. Vasilopoulos, G. Pavlakos, K. Schmeckpeper, K. Daniilidis, and D. E. Koditschek, “Reactive navigation in partially familiar planar environments using semantic perceptual feedback,” *Int. J. Robot. Res.*, vol. 41, no. 1, pp. 85–126, 2022.

[16] S. G. Loizou, “The navigation transformation,” *IEEE Trans. Robot.*, vol. 33, no. 6, pp. 1516–1523, Dec. 2017.

[17] P. Vlantis, C. P. Bechlioulis, and K. J. Kyriakopoulos, “Robot navigation in complex workspaces employing harmonic maps and adaptive artificial potential fields,” *Sensors*, vol. 23, 2023, Art. no. 4464.

[18] D. Guralnik, P. Stiller, F. Zegers, and W. E. Dixon, “Distributed cooperative navigation with communication graph maintenance using single-agent navigation fields,” in *Proc. Amer. Control Conf.*, 2022, pp. 2160–2165.

[19] I. F. Filippidis and K. J. Kyriakopoulos, “Navigation functions for everywhere partially sufficiently curved worlds,” in *Proc. IEEE Int. Conf. Robot. Autom.*, 2012, pp. 2115–2120.

[20] D. E. Koditschek and E. Rimon, “Robot navigation functions on manifolds with boundary,” *Adv. Appl. Math.*, vol. 11, no. 4, pp. 412–442, Dec. 1990.

[21] S. Paternain, D. E. Koditschek, and A. Ribeiro, “Navigation functions for convex potentials in a space with convex obstacles,” *IEEE Trans. Autom. Control*, vol. 63, no. 9, pp. 2944–2959, Sep. 2018.

[22] H. Kumar, S. Paternain, and A. Ribeiro, “Navigation of a quadratic potential with ellipsoidal obstacles,” in *Proc. IEEE Conf. Decis. Control*, 2019, pp. 4777–4784.

[23] Z. Kan, E. Doucette, and W. E. Dixon, “Distributed connectivity preserving target tracking with random sensing,” *IEEE Trans. Autom. Control*, vol. 64, no. 5, pp. 2166–2173, May 2019.

[24] Y. Kim and M. Mesbahi, “On maximizing the second smallest eigenvalue of a state-dependent graph Laplacian,” *IEEE Trans. Autom. Control*, vol. 51, no. 1, pp. 116–120, Jan. 2006.

[25] P. Ong, B. Capelli, L. Sabattini, and J. Cortes, “Nonsmooth control barrier function design of continuous constraints for network connectivity maintenance,” *Automatica*, vol. 156, 2023, Art. no. 111209.

[26] O. Arslan, D. P. Guralnik, and D. E. Koditschek, “Coordinated robot navigation via hierarchical clustering,” *IEEE Trans. Robot.*, vol. 32, no. 2, pp. 352–371, Apr. 2016.

[27] H. G. Tanner and A. Kumar, “Formation stabilization of multiple agents using decentralized navigation functions,” in *Proc. Robot., Sci. Syst.*, 2005, pp. 49–56.

[28] Z. Kan, A. Dani, J. M. Shea, and W. E. Dixon, “Ensuring network connectivity during formation control using a decentralized navigation function,” in *Proc. IEEE Mil. Commun. Conf.*, San Jose, CA, USA, 2010, pp. 954–959.

[29] M. Mesbahi and M. Egerstedt, *Graph Theoretic Methods in Multiagent Networks*, vol. 33. Princeton, NJ, USA: Princeton Univ. Press, 2010.

[30] W. Ren, “Consensus based formation control strategies for multi-vehicle systems,” in *Proc. IEEE Amer. Control Conf.*, Minneapolis, MN, USA, 2006, pp. 4237–4242.

[31] A. Rantzer, “A dual to Lyapunov’s stability theorem,” *Syst. Control Lett.*, vol. 42, no. 3, pp. 161–168, 2001.

[32] G. Notomista and M. Severiano, “Safety of dynamical systems with multiple non-convex unsafe sets using control barrier functions,” *IEEE Control Syst. Lett.*, vol. 6, pp. 1136–1141, 2022.

[33] F. Blanchini, “Set invariance in control,” *Automatica*, vol. 35, no. 11, pp. 1747–1767, 1999.

[34] J.-M. Bony, “Principe du maximum, inégaliteé de Harnack et uniceité du problème de Cauchy pour les opérateurs elliptiques dégénérés,” *Annales de L’Institut Fourier*, vol. 19, no. 1, pp. 277–304, 1969.

[35] H. Brezis, “On a characerization of flow-invariant sets,” *Commun. Pure Appl. Math.*, vol. 23, pp. 261–263, 1970.

[36] W. N. Anderson and T. D. Morley, “Eigenvalues of the Laplacian of a graph,” *Linear Multilinear Algebra*, vol. 18, no. 2, pp. 141–145, 1985.

[37] B. V. Dekster, “The Jung theorem in metric spaces of curvature bounded above,” *Proc. Amer. Math. Soc.*, vol. 25, no. 8, pp. 2425–2433, Aug. 1997.

Dan P. Guralnik received the B.A., M.Sc., and Ph.D. degrees in mathematics from the Technion–IIT, Haifa, Israel, in 1994, 1998, and 2005, respectively.

Trained in geometric group theory, in 2011 he made a transition from pure mathematics into robotics with KodLab, University of Pennsylvania. He is now a Research Scientist with the Non-Linear Control and Robotics Lab, Mechanical and Aerospace Engineering Department, University of Florida, Gainesville, FL, USA. His research interests include applications of geometry and topology to hybrid and multiagent systems, to knowledge representation and machine learning, and in the development of compositional methods for hybrid control.

Peter F. Stiller received the undergraduate degree in mathematics and economics from MIT, Cambridge, MA, USA, in 1973 and the Ph.D. degree in mathematics from Princeton University, Princeton, NJ, USA, in 1977.

He is currently a Professor of Mathematics with Texas A&M University, College Station, TX, USA. His early work was in algebraic geometry; later branching out into applications of algebraic and differential geometry to problems in geometric modeling, robotics, computer vision, and artificial intelligence. He has held year long visiting positions with the Institut des Hautes Etudes Scientifiques (twice), the Max- Plank-Institut fur Mathematik in Bonn, the Institute for Advanced Study in Princeton, and the Mathematical Sciences Research Institute in Berkeley. In addition he has held short term positions with various government labs, including the former Army High Performance Computing Research Center, the David Taylor Naval Research Lab, and the Air Force Research Lab with Wright Patterson AFB. He is the author of some 60 scientific publications and 17 technical reports.

Federico M. Zegers (Member, IEEE) received the Ph.D. degree in mechanical engineering from the Department of Mechanical and Aerospace Engineering, University of Florida, Gainesville, FL, USA, in 2021.

He is currently a Senior Professional Staff I with the Johns Hopkins University Applied Physics Laboratory, Laurel, MD, USA, where he continues to conduct research on robotics, hybrid dynamical systems, nonlinear and adaptive control, and multiagent systems.

Warren E. Dixon (Fellow, IEEE) received the Ph.D. degree in electrical engineering from Clemson University Clemson, SC, USA, in 2000.

After working with Oak Ridge National Laboratory as a Wigner Fellow and Research Staff Member, he joined the University of Florida, Gainesville, FL, USA, in 2004 and is now the Dean’s Leadership Professor and Department Chair with the Department of Mechanical and Aerospace Engineering. His main research interests include the development and application of Lyapunov-based control techniques for uncertain nonlinear systems.

Dr. Dixon is an ASME Fellow for contributions to adaptive control of uncertain nonlinear systems. His work has been acknowledged by various early and mid-career awards and best paper awards.